Dynamic metabolism between the retinal pigmented epithelium and retina reveals a metabolic ecosystem in the eye

Mark Akio Kanow

A dissertation
submitted in partial fulfillment of
the requirements for the degree of

Doctor of Philosophy

University of Washington

2019

Reading Committee:

James B. Hurley, Chair
Hannele Ruohola-Baker
Thomas Reh

Program Authorized to Offer Degree:

Biochemistry

University of Washington

Abstract

Dynamic metabolism between the retinal pigmented epithelium and retina reveals a metabolic ecosystem in the eye

Mark Akio Kanow

Chair of the Supervisory Committee:

Professor James B. Hurley

Biochemistry

There are a collection of specialized neurons and glia in the retina that convert visible light that enters the eye into chemical signals that stimulate biological processes that contribute to our visual perception. Photoreceptors are the light sensitive neurons of the retina that kickoff this process. They are a highly polarized cell that must produce large amounts of energy to maintain their polarity and detect the absence or presence of light. There exist metabolic adaptations between them, the retinal pigmented epithelium (RPE) and Müller glia cells (MGCs) of the retina. These metabolic adaptations enhance the flow of glucose from the choroid through the RPE to rod and cone photoreceptors to promote retinal function and survivability. In age-related, or inherited retinal diseases such as retinitis pigmentosa, it's been observed that photoreceptor degeneration and death occurs when these specific metabolic adaptations are disturbed.

We investigated a metabolic flux model in photoreceptors and the RPE using a variety of analytical techniques that include: mass spectrometry, confocal immunofluorescence

imaging, and animal imaging of mouse and zebrafish retina and cultured human fetal RPE cells (hfRPE). In our model, we found that considerable amounts of glucose traverse through the RPE in mouse and zebrafish eye towards the retina, and that glucose enters the retina through photoreceptors. Photoreceptors are highly glycolytic and convert the glucose into lactate to meet their energy demands. Photoreceptor lactate can then be exported to the RPE and neighboring MGCs. We used cultured human fetal RPE cells to identify that lactate can suppress the consumption of glucose by the RPE to allow for its utilization by the retina. With the consumption of glucose suppressed in the RPE, it can allow for increased amounts of glucose to reach the retina from the choroidal blood supply. Additionally, we identified that the RPE is capable of storing excess glucose in the form of glycogen possibly for feeding the retina when circulating glucose levels are low. Altogether, these findings provide a foundation for understanding the metabolic relationships in the retina that can be applied towards new concepts of novel strategies for preventing photoreceptor degeneration and blindness.

Table of Contents

List of Figures

Glossary

2-NBDG: (2-(*N*-(7-Nitrobenz-2-oxa-1,3-diazol-4-yl)Amino)-2-Deoxyglucose)
GAP: glyceraldehyde-3-phosphate
GAPDH: glyceraldehyde-3-phosphate dehydrogenase
GC-MS: gas chromatography-mass spectrometry RPE: Retinal pigment epithelium
Gln: glutamine
GLUT: glucose transport protein
GFP: green fluorescent protein
GS: glutamine synthetase
hfRPE: human fetal RPE
IB: immunoblot
IHC: immunohistochemistry
INL: inner nuclear layer
IPL: inner plexiform layer
LC-MS/LCMS: liquid chromatography mass spectrometry
LDH: lactate dehydrogenase
mEC: mouse eyecup
MGC(s): Müller glial cell(s)
MT-COX1: mitochondrial cytochrome C oxidase
mRetina: mouse retina
Nrl: neural retina-specific leucine zipper promoter
ONL: outer nuclear layer
OPL: outer plexiform layer
OS: outer segment
PK: pyruvate kinase
PKM2: pyruvate kinase isoform M2
PR: photoreceptor
Pro: proline
Pyr: pyruvate
Rlbp: retinaldehyde binding protein promoter
RPE: retinal pigment epithelium
SD: standard deviation
SE: standard error of the mean
SEM: scanning electron microscopy
TCA: tricarboxylic acid
tdTomato: tandem dimeric tomato fluorescent protein

Acknowledgments

Jim Hurley provided me with ample room to take chances and make mistakes, but was always available to help me out when things got messy. His guidance and input have been crucial to my development as a scientist, and helped elevate my graduate school experience beyond the common and simple science project. Looking back at my time in Jim's lab, I'm in shock and awe at how much I've learned. Also, many thanks to my thesis committee (Susan Brockerhoff, Steve Hauschka, Thomas Reh, and Hannele Ruohola-Baker). Everyone provided invaluable knowledge and experience towards captivating discussions and experiments.

A lot of this work would not have been possible without the help of fellow lab members and collaborators who were unselfish with their time and reagents. Jon Linton, Jianhai Du, Ashley George, Ken Lindsay, Whitney Cleghorn, Sara Hayden, Connor Jankowski, Abbi Engel, Jennifer Chao, Kaitlin Knight, Chris Farnsworth, the labs of Ian Sweet and Tom Reh, Rachel Hutto, Kristine Tsantilas, and Celia Bisbach cultivated a lot of ideas that helped inspire many experiments. James Kuchenbecker, Dan Possin, Jing Huang, Ed Parker, and Dale Cunningham in the UW Vision Core contributed a lot to providing training in tissue preparation and fixation for confocal imaging. One of the lab's bread & butter techniques for investigating retina metabolism is mass spec, and Martin Sadilek who manages the Mass Spec Facility in the UW Chemistry Department was essential for teaching and training me in the techniques of LCMS and GCMS.

Graduate school can make your head feel stripped just like a screw that's been tightened too many times, and having a strong supportive network of friends and family helps shield you from the waves. Michelle Henry-Stanley imparted a lot of brutally honest words of wisdom that helped me navigate academia successfully. "Thank You, Shawn Pooparnthong." You helped put a lot of things into perspective and provided welcomed distractions when I was working too much, and I'd prefer it if you were alive and well today to keep up with the distractions. Lastly, the long days of failed experiments can be grueling, and I am indebted to my Buttery Bisque and Cowa Bacon-Jaybers for dragging me up when I was down. You two are the sun, too good to be true, and I am just the planets spinning around you. Many thanks go to you two for brightening my life, and making the graduate school journey enjoyable.

Dedication

This dedication is split seven ways to Rebecca, Cora, Mom, Dad, Paul, and Aaron.
As eloquently said by,
Shaq, Charles Barkley, and Kenny Smith,
“We never lose! We never lose! We never lose!”

Chapter 1

Introduction

Structure of the eye and retina

Vision is a valuable ability, and it's easy to accept why this is the case given the framework of daily life. Our eyes play a major role in our worldly interactions from feeding ourselves to learning. Key structural and cellular features of the eye lend themselves to our visual perception. In the outer most vasculature of the eye lies the choroid between the sclera and retina pigmented epithelium (RPE) (INSERT Fig.1.1). The retina is the light-detecting tissue at the back of the eye of most vertebrate organisms (Kolb 1991, Kolb 2005). Adjacent to the choroid is the RPE, which is composed of a monolayer of polarized and pigmented cells joined together by tight junctions. The RPE prevents diffusion by serving as a selective blood-retina barrier between the choroid and the outer segments of photoreceptors (PR). Additionally, RPE cells support phototransduction by providing photoreceptors with 11-cis retinal, which is needed for the absorption of light (Strauss 2005). Any scattered light that is not absorbed by photoreceptors is absorbed by RPE cells to help improve optical quality, and limit any photo-oxidative stress caused by the un-absorbed light. The RPE makes contact with the tips of photoreceptor outer segments to form apical processes that intercalate between photoreceptor outer segments (OS) of the retina (Bonilha 2014).

The retina is the light-detecting tissue at the back of the eye of most vertebrate organisms (Kolb 1991, Kolb 2005). Photoreceptor OS capture the light that enters the eye with light sensitive structures that convert the photons into an electrical-chemical signal that is interpreted by bipolar, horizontal, and amacrine cells. There are two varieties of photoreceptors that detect the light that enters our eyes, rods and cones. Although they differ slightly, they both have similar structures and absorb photons to kick off the visual response that ends in the perception of an image. Rods are specialized for the detection of low light levels, and cones are sensitive to bright light and color acumen. Photons are absorbed by light sensitive chromophores that are

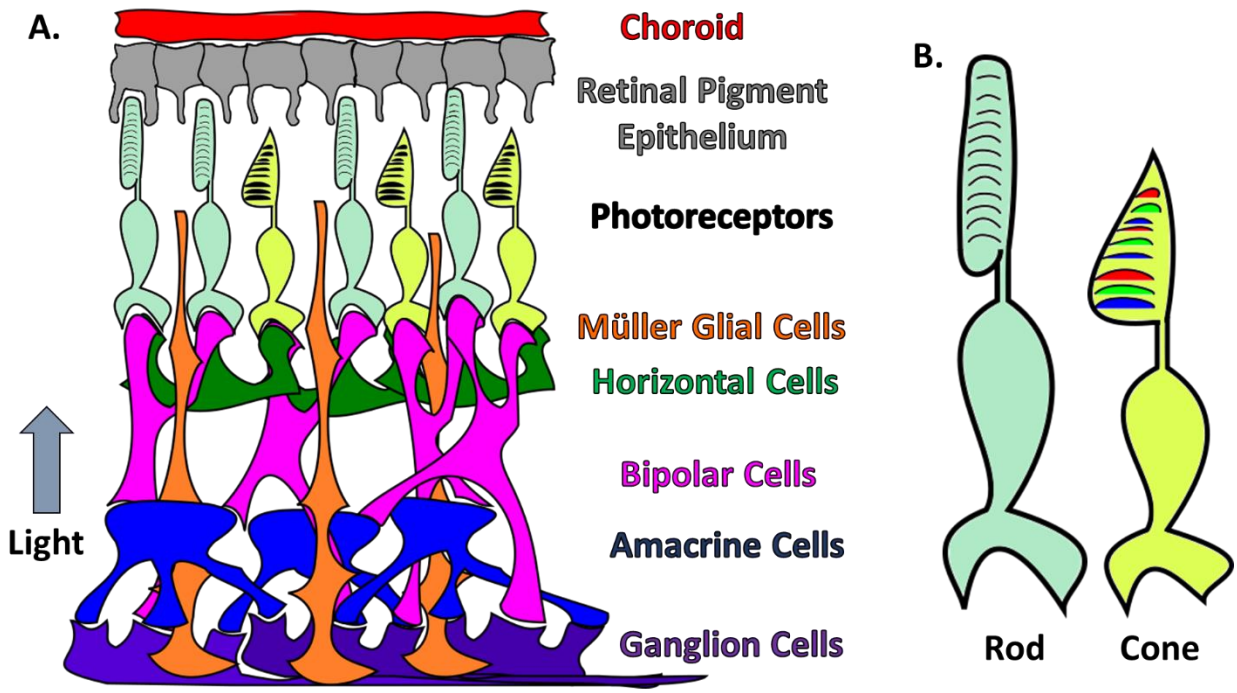

Fig. 1.1. Schematic of the (A) retina and (B) photoreceptors.

bound to transmembrane proteins in the membranous disks that are housed in the OS of photoreceptors (Heitzmann 1972, Papermaster and Dreyer 1974). For rods, rhodopsin is the light sensitive protein; cones use a similar opsin to capture the different wavelengths of color light. All photoreceptors contain an inner segment which houses mitochondria, endoplasmic reticulum, and the nucleus. The last tier of the photoreceptor is the synapse. Photoreceptors have a ribbon synapse, which differs from other synapses in the body. It holds primed neurotransmitter vesicles that are coupled to changing calcium concentrations which allows for rapid neurotransmitter release and sustained signal transmission onto bipolar cells (Sterling and Matthews 2005).

Another key cell type of the retina are Müller glia cells (MGCs). They are a specialized type of glial cell that constitute about 90% of all retinal glia, and they radially extend across the retina from the ganglion cell layer to the PR inner segments (IS) (de Melo Reis et al., 2008). They form an organized scaffold network that ensheathes retinal neurons along their path to provide stability to the complex framework of the adult retina. They form adherens junctions with photoreceptors, and contribute to the functional pH and ion homeostasis of the retina (Reichenback et al., 2013). The collective effort of these different neurons and cells help propagate the light induced signals from

photoreceptors to downstream ganglion cells whose axons form the optic nerve that extends towards and into the brain. Information from both retinas travels through the optic nerve to the visual cortex of the brain where the information is translated into an image.

RPE, photoreceptor, and MGC contributions to retina metabolism

The cells of the RPE are joined by tight junctions and serve as a selective barrier between the choroidal blood supply and the retina. The RPE has a variety of roles in the retina, but an essential role is its contribution to retinal metabolism. It can transport glucose and has monocarboxylate transporters (MCTs) needed for nutrient and waste removal to and from the retina (Yoon et. al. 1997, Bergersen et. al. 1999). The RPE also transports ions and fluid from the interphotoreceptor matrix (IPM) that surrounds retinal photoreceptors to the choroid (Adijanto et. al. 1997). This allows for the exchange of metabolites between the RPE and photoreceptors (Strauss 2005). Other critical roles for the RPE include: processing retinal into 11-cis-retinal (Lamb and Pugh 2004), phagocytizing photoreceptor outer segments that are shed as a result of light induced phototransduction (Kevany and Palczewski 2010), and the excretion of neurotrophic factors that promote PR stabilization and survival (Steele et al., 1993).

RPE tight junctions allow for it to serve as the blood-retina barrier between the choroid and the retina, and allow for selective diffusion of nutrients from the blood supply to the retina. Glucose from the choroidal blood supply is the immediate energy substrate of the retina, and must diffuse across the RPE for photoreceptor consumption. It enters PR through specialized glucose transporters (GLUTs) (Kanow et al,. 2017), and is phosphorylated by hexokinase to make glucose-6-phosphate in photoreceptors. Glucose 6-phosphate can enter glycolysis, the pentose phosphate pathway or glycogenesis. Glucose is mainly processed via glycolysis in the retina via a hexokinase-II that is present in photoreceptors (Rajata et al., 2013, Du et al., 2013, Winkler 1981, Lowry et al., 1961). Phosphofructokinase, glucose 6-posphate dehydrogenase, and pyruvate kinase have been localized to photoreceptors (Lowry et al., 1961, Lindsay et al., 2014).

Müller glia cells have many contributions to retina metabolism. As previously mentioned, they have the ability to transport monocarboxylates, glucose, and amino acids to and from cells in the retina (Reichenback et al 2013). They are the sole contributors to glutamine synthesis in the retina (Bringmann et al 2009). Glutamate is the primary excitatory neurotransmitter of the vertebrate retina. Retinal neurons will synthesize glutamate from Müller cell glutamine in order to sustain sufficient levels of glutamate for neurotransmission (Bringmann et al 2009, Thoreson and Witkovsky 1999). If glutamine synthesis is blocked, neurotransmission cannot occur and glutamate accumulates, which is toxic to neurons (Bringmann et al 2009). In addition to glutamine synthesis, Müller cells also possess the ability to synthesize and breakdown glycogen (PérezLeón et. al 2013, Pfeiffer et al 2005, and Rothermel et al 2008). The distribution and amount of glycogen stored has an inverse relationship with respect to the extent of retinal blood supply (Kuwabara et al 1961). Species like the guinea pig and rabbit, which have avascular retinas store the most glycogen. The majority of this glycogen is stored within Müller cell end feet (Shimizu et. al 1953). *In vitro* studies have indicated that glycogen storage/synthesis may be regulated by an insulin-signaling pathway in the retina as well as in primary cultures of Müller cells (PérezLeón et. al 2013) (Fig. 1.2 illustrates a summary of some of the metabolic pathways between PRs and MGCs).

There is some evidence that gluconeogenesis can occur in Müller cells. They may be able to use lactate (Goldman et al 1986, Goldman et al 1987) to make glucose for incorporation into glycogen (Goldman 1988). Primary Müller cell cultures from amphibian retinas still exhibit this fuel preference for the gluconeogenic pathway, and it was suggested that there is a “Cori-like” cycle in the retina where Müller cells utilize excess lactate to synthesize glucose that is stored as glycogen which is then used to supply glucose to other cells in the retina (Goldman 1990). Müller cells express enolase, a required enzyme for gluconeogenesis, and express low/nonexistent levels of any isoform of pyruvate kinase (PKM2) (Lindsay et. al. 2014). This deficiency in PKM2 and presence of enolase may reflect a gluconeogenic pathway in Müller cells.

Müller glia may influence retinal vascular diseases such as retinopathy of prematurity, diabetic retinopathy, and age-related macular degeneration (Coorey et. al. 2012). In diabetic retinopathy, Müller cells demonstrate impaired uptake of glutamate and glutamine synthesis (Li, Q. et. al. 2002). A better understanding of their metabolic contributions to the retina may provide new therapies for treating retinal vascular diseases.

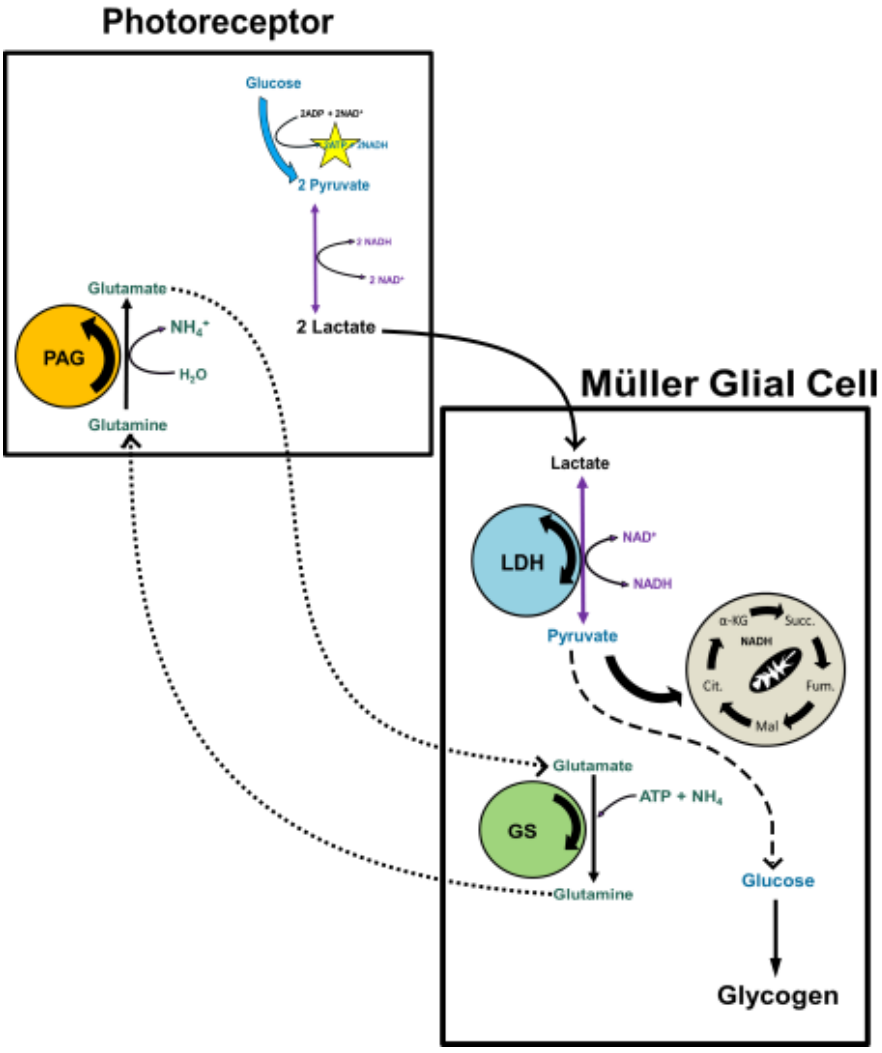

Fig. 1.2. Schematic summary of glycolysis, glutamine recycling, TCA cycle (oxidative phosphorylation), and glycogen storage between photoreceptors and Müller glial cells.

Photoreceptor and RPE metabolism in retinal disease

Photoreceptors and RPE have distinct metabolic differences. Whereas photoreceptors rely on aerobic glycolysis to meet their energy demands, the RPE relies more on mitochondrial respiration for producing ATP (Chao et al 2017; Kanow et al., 2017).

Recent studies have found that the flux of glucose through glycolysis promotes the survival of cone photoreceptors in a retinal disease model of retinitis pigmentosa where photoreceptors degenerate, ultimately leading to blindness (Ait-Ali, et. al. 2015., Zhang, et. al. 2016). In one study, a thioredoxin secreted by rod photoreceptors, Rod-derived cone viability factor (RdCVF), protects cones from degeneration by acting through a transmembrane protein Basigin-1 (BSG1). BSG1 stabilizes a glucose transporter (GLUT1) in cone photoreceptors. Another study showed that enhancing expression of glycolytic genes in photoreceptors protects them from degeneration induced by altered cGMP metabolism (Zhang, et. al. 2016). When RPE metabolism is genetically altered to favor glycolysis, photoreceptors are observed to degenerate leading to blindness (Zhao et. al., 2011).

Furthermore, a disease model of retinitis pigmentosa showed that supplementing glucose to PRs *in vivo* restored cone photoreceptor function and survivability, restoring vision (Want et al., 2016). The same study found that a fluorescent derivative of glucose, 2-deoxy-D-glucose (2-NBDG), was sequestered in the RPE when rod photoreceptors were degenerating. Photoreceptors are the primary manufacturers of retinal lactate that can be utilized by the RPE for oxidative phosphorylation, and lactate levels are significantly diminished when rods degenerate (Lindsay et al., 2014; Kanow et al., 2017). Altogether, these studies bring to light that metabolic specialization exists in the eye and retina, and when these specializations are disrupted it can lead to vision lost. It was the aim of my studies to explain and understand these findings by defining a novel model for the RPE/PR and PR/MGC metabolic relationships that contribute to the function of the retina.

Chapter 2

Biochemical adaptations of the retina and retinal pigment epithelium support a metabolic ecosystem in the vertebrate eye

Introduction

Mutations in any of more than140 genes can cause photoreceptors in a vertebrate retina to degenerate (Bramall et al., 2010). The relationship between photoreceptor degeneration and the diversity of biochemical functions and expression patterns of those genes is enigmatic. The diversity suggests that the consequences of loss or gain of function of these genes may converge onto a few essential metabolic processes (Punzo et al., 2009; Zhang et al., 2016). Much has been gained by studying specific functions of the genes and therapeutic strategies for specific genetic deficiencies are being developed (Sengillo et al., 2017). Nevertheless, a more general understanding of what photoreceptors need to survive could suggest therapeutic strategies that are more broadly applicable. With that in mind, we have been investigating the fundamental nature of energy metabolism in the retina and the retinal pigment epithelium (RPE) (Du et al., 2013a; 2013b; 2015; 2016a; 2016b; Lindsay et al., 2014; Linton et al., 2010).

Glucose that fuels the outer retina comes from the choroidal blood. Before it can reach the retina, however, it first must traverse the RPE. The RPE is a monolayer of polarized cells between the choroid and retina that functions as a blood-retina barrier. Cells in the RPE, bound together by tight junctions, express specific transporter proteins on their basolateral and apical surfaces (Lehmann et al., 2014). Glucose from the choroid passes through transporters on the basolateral surface, and then wends its way through the cytoplasm of the RPE cell. If metabolic enzymes within the RPE cell do not consume it, the glucose moves down a concentration gradient toward the opposite side of the RPE cell where it exits to the retina through transporters on the apical surface of the RPE.

Most of the glucose that reaches the retina is consumed by glycolysis and converted to lactate. Retinas and tumors were two of the tissues identified in the 1920’s by Warburg

and Krebs (Krebs 1927; Warburg et al., 1924) as relying mostly on “aerobic glycolysis”. This type of metabolism can release massive amounts of lactate from a cell even when O_2 is available. Evidence indicates that photoreceptors in the outer retina are the site of aerobic glycolysis (Du et al., 2016a; Lindsay et al., 2014; Chinchore et al., 2017; Medrano and Fox 1995; Wang et al., 1997; Winkler 1981). The importance of aerobic glycolysis for survival and function of photoreceptors is not yet clear, but several investigators have proposed that it enhances anabolic activity within photoreceptors (Zhang et al., 2016; Chinchore et al., 2017; Rajala et al., 2016; Rueda et al., 2016; Venkatesh et al., 2015.).

Energy metabolism is strikingly different in RPE cells than in the retina. Recently, we showed that RPE cells are specialized for a type of energy metabolism called reductive carboxylation (Du et al., 2016b) that aids in redox homeostasis. In general, RPE cells appear to rely more on their mitochondria.

Recent reports described genetic manipulations that explored the effects of qualitatively altering energy metabolism either in photoreceptors or in RPE cells *in vivo*. Glycolysis in rods was enhanced in one study by blocking expression of SIRT6 (Zhang et al., 2016). Another study enhanced glycolysis in cones by activating mTORC1 (Venkatesh et al., 2015). Those studies indicated that making photoreceptors more glycolytic makes them more robust. Both strategies slowed degeneration of photoreceptors in retinas where rods were degenerating as a consequence of a mutation associated with retinitis pigmentosa (Zhang et al., 2016; Venkatesh et al., 2015). Conversely, photoreceptors degenerate when RPE cells are made more glycolytic *in vivo.* When glycolysis in the RPE was enhanced by knocking out VHL (Kurihara et al., 2016) or by knocking out an essential mitochondrial transcription factor in RPE cells *in vivo* (Zhao et al., 2011) the neighboring photoreceptors died.

The findings of those *in vivo* studies appear puzzling and seemingly contradictory when considered only from a cell autonomous perspective. Why does enhancing glycolysis benefit some cells and endanger others? Here we propose that those findings make

more sense when interpreted in the context of metabolic relationships between the retina and the RPE. We describe evidence that the retina and RPE function as a metabolic ecosystem. We show that photoreceptors are the main point of entry for glucose into the retina. They convert glucose to lactate, which then serves as a fuel for neighboring cells in the retina. We report that lactate can suppress glycolysis in RPE cells and thereby protect glucose so that more of it can reach the retina. The model that we propose based on these findings predicts that each cell in the retina and RPE contributes an essential metabolic function that promotes survival of the entire retina-RPE ecosystem.

Results

Photoreceptors express a glucose transporter

Uptake of glucose into cells requires a protein that can transport glucose. We used immunoblotting of mouse tissues to evaluate expression of glucose transporters (Fig. 2.1A) and confirmed previous findings (Badr et al., 2000; Gospe et al., 2010) that retina and RPE express GLUT1. We confirmed that the GLUT1 immunoreactive protein was membrane associated (Fig. 2.1B). GLUT3 was detected only in brain. GLUT4 was detected in heart and muscle as expected, but not in the retina.

Fluorescent immunohistochemistry (IHC) and confocal microscopy of mouse retinas shows that GLUT1 immuno-reactivity overlaps with cytochrome oxidase subunit 1 (MT-CO1) (Fig. 2.1C), which identifies rod inner segments by the unique elongated shape of their mitochondria (Fig 2.1E). These mitochondria extend beyond and are absent in the ends of the Müller glial cell (MGC) apical processes (Fig 2.1E). Instead, small spherical-shaped mitochondria line up within the MGCs along the outer limiting membrane, just beneath the apical processes (Fig. 2.1F and arrowheads in Fig. 2.1C). MGCs, labeled with an antibody to glutamine synthetase (GS) in Fig. 2.1D, extend from the outer limiting membrane to the ganglion cell side of the retina. Most GLUT1 immunoreactivity in MGCs is in the inner retina (Fig. 2.1D). GLUT1 immunoreactivity also overlaps with a marker specific for rod photoreceptors (rod arrestin, Fig. 2.1G), and it overlaps with GFP expressed from the rod-specific Nrl promoter (Fig. 2.1H). Taken altogether, the

distribution of GLUT1 immunoreactivity supports the idea that photoreceptors can take up glucose released from the apical side of the RPE.

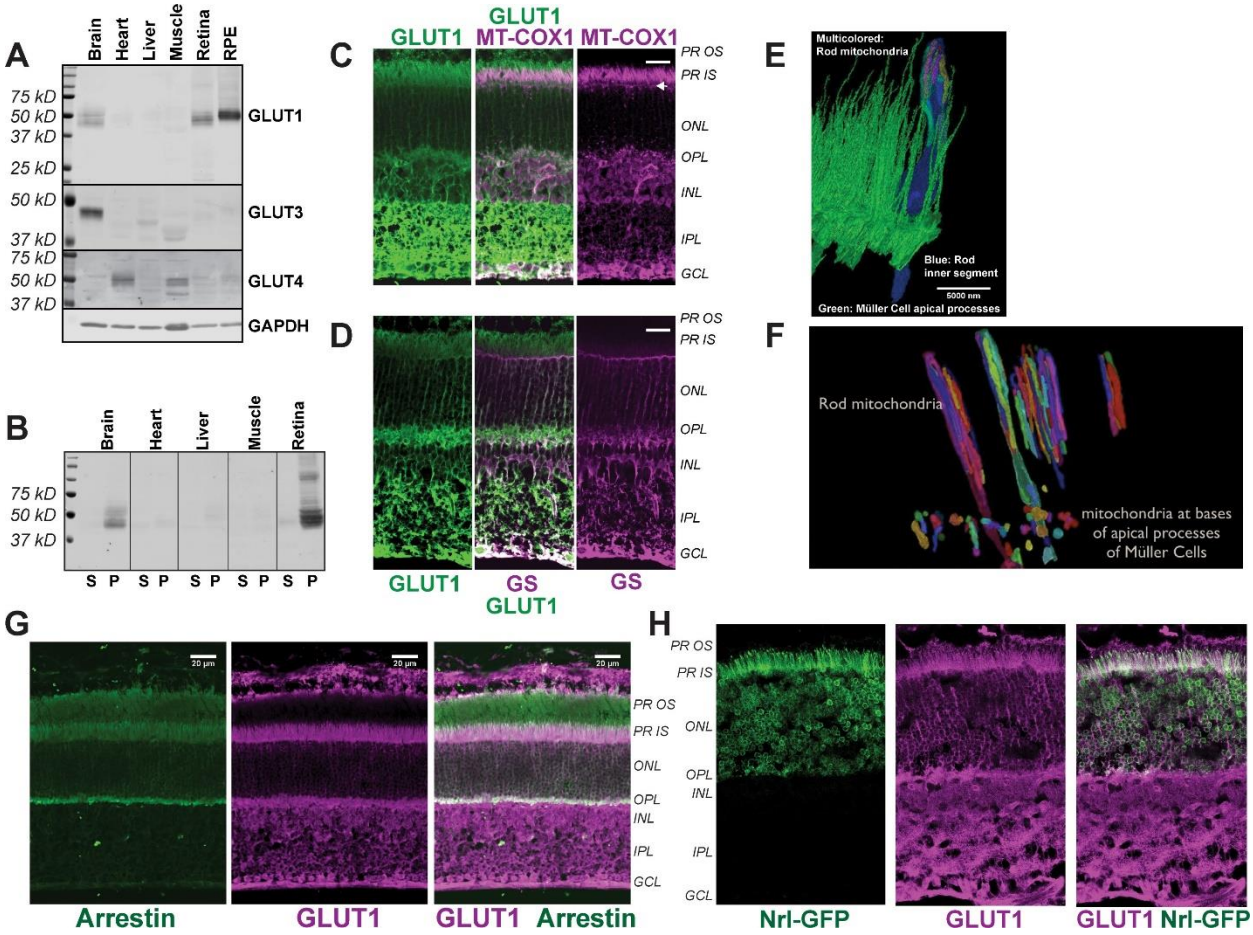

Figure 2.1. Distribution of GLUT1 in retina. **(A)** Immunoblot analysis of mouse tissue homogenates confirms GLUT1 is a major glucose transporter in mouse retina and RPE. 1 µg protein was loaded in each lane. No antibodies that we could validate were available for GLUT2. The Human Protein Atlas reports no expression of GLUT2 in retina (Uhlén et al., 2015). The presence of GLUT4 in RPE requires confirmation by IHC, but this antibody produces high background not suitable for IHC. The blot shown is representative of 3 experiments. **(B)** Evidence that the protein immunoreactive with the GLUT1 antibody is membrane associated. Homogenates were centrifuged and equivalent percentages of total supernatant (S) and total pellet (P) were probed with the GLUT1 antibody. **(C)** GLUT1 in mouse retina. Rod inner segments are identified by the unique morphology of their mitochondria labeled with mitochondrial cytochrome oxidase one antibody (MT-COX1). White arrowhead indicates the layer of Müller cell mitochondria. **(D)** Müller cells are identified by glutamine synthetase (GS) immunoreactivity. **(E)** Serial Block Face Scanning Electron Microscopy. The inner segment of one rod cell is shown in blue with its mitochondria shown as multi-colored. The green structures are apical processes of MGCs. **(F)** Differences in location and morphology between rod mitochondria and MGC mitochondria in mouse retina. For clarity not all of the mitochondria are shown. MGC mitochondria are located just below

the outer limiting membrane. **(G)** Left panel shows labeling of rods in a partially light-adapted mouse retina with a rod arrestin antibody. Middle panel shows labeling with a GLUT1 antibody and right panel shows the merge. **(H)** Left panel shows expression of GFP from the rod-specific Nrl promoter. The middle panel shows labeling with a GLUT1 antibody and the right side shows the merge. PR OS, photoreceptor outer segment; PR IS photoreceptor inner segment; ONL, outer nuclear layer; OPL, outer plexiform layer; INL inner nuclear layer; IPL inner plexiform layer; GCL, ganglion cell layer. Scale bars in C, D, and G represent 20 μm.

Dietary glucose enters the retina primarily through photoreceptors.

Next we asked which cells in the retina take up glucose in the context of an eye within a living animal. We used oral gavage to introduce a fluorescent derivative of 2-deoxy glucose (2-NBDG) (Yoshioka et al., 1996) into stomachs of mice. We harvested the retinas either 20 or 60 minutes after gavage, mounted them on filter paper and cut 300-400 μm slices for imaging by confocal microscopy (Giarmarco et al., 2017). Fig. 2.2A shows that 2-NBDG fluorescence is strongest in the photoreceptor layer, suggesting that photoreceptors are the first cells in the retina to take up glucose from the choroid vasculature. Surprisingly, 2-NBDG fluorescence is stronger in the outer retina than in the inner retina even though mouse inner retinas are vascularized. We noted that 2-NBDG fluorescence does not overlap with MGC's, which were labeled in these experiments by transgenic expression of tdTomato (Wohl and Reh 2016), though in rare instances there was little overlap at MGC end feet. These results are summarized and quantified in Fig. 2.2C. They show that glucose that reaches the outer retina is taken up primarily by photoreceptors. There appears to be little overlap of the NBDG signal with the tdTomato label in MGC's.

The images in Fig. 2.2A were made from live, unfixed mouse retinas. Most photoreceptors in mouse retinas are rods. It is difficult in these images to resolve whether cones also import 2-NBDG. To address this we also introduced 2-NBDG by oral gavage into adult zebrafish, whose retinas are more enriched with cones (Raymond et al., 2014). Fig. 2.2B shows that cones become intensely fluorescent 30 minutes after gavage. As in mouse retinas, there was no indication of fluorescent glucose uptake into MGCs, which in these retinas were marked with tdTomato expressed from a GFAP

promoter (Shin et al., 2014). Fig. 2.2D reports quantification and summarizes the zebrafish retina results.

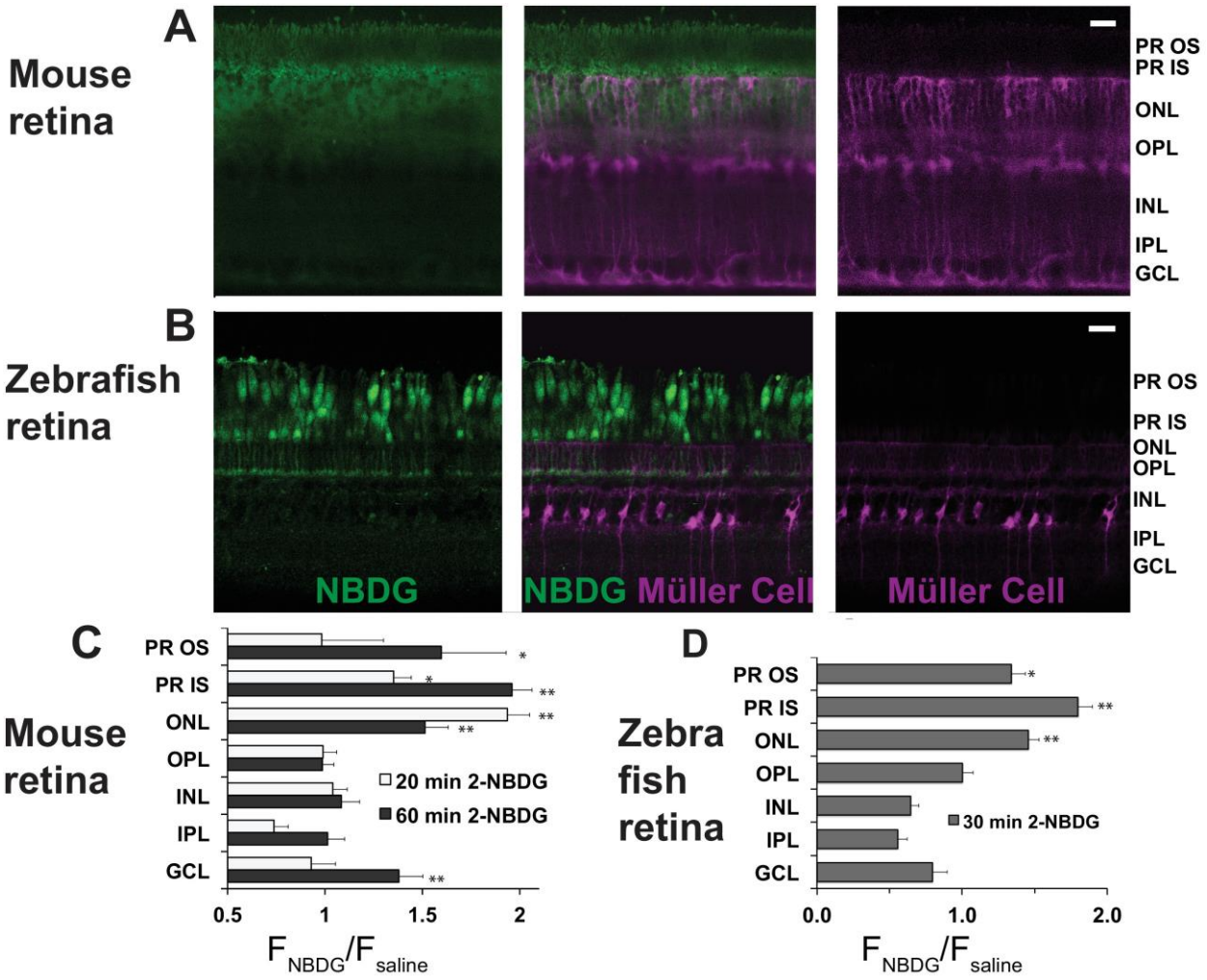

Fig. 2.2. Fluorescent glucose (2-NBDG) accumulates in photoreceptors after oral gavage. **(A)** 2-NBDG (green) accumulation in a mouse retina 20 min. after oral gavage. MGCs are identified by tdTomato in cells in which the Rlbp1 promoter is active. **(B)** 2-NBDG accumulation in a zebrafish retina 30 min after oral gavage. MGCs are identified by tdTomato expressed from the GFAP promoter. Labels on the right of panels A and B represent approximate positions of the retinal layers, **(C)** Quantification of 2-NBDG fluorescence from mouse retinas (n = 5 animals, 17 slices for 20 min 2-NBDG; 3 animals, 8 slices for 1 h 2-NBDG; 3 animals, 8 slices for saline). F_{NBDG}/F_{saline} compares fluorescence from retinas of mice gavaged with 2-NBDG vs. with saline. Error bars report SE. **(D)** Quantification of 2-NBDG fluorescence from zebrafish retinas (3 animals, 8 slices for 30 min 2-NBDG; 2 animals, 3 slices for saline). PR OS, photoreceptor outer segments; PR IS, photoreceptor inner segments; ONL, outer nuclear layer; OPL, outer plexiform layer; INL, inner nuclear layer; IPL, inner plexiform layer; GCL, ganglion cell layer. Scale bars represent 20 μm. * indicates $p < 0.05$ and ** indicates $p < 0.01$ for the comparison of F_{NBDG} to F_{saline}.

Glucose is metabolized differently in RPE cells than in retina.

Previous studies showed that most of the glucose taken up into a retina is used to make lactic acid (Du et al., 2016a; Krebs 1927; Warburg et al., 1924; Medrano and Fox 1995; Wang et al., 1997; Winkler 1981). Within the eye of a living animal, glucose from the choroidal blood first must pass through the monolayer of RPE cells before it can reach the retina. We hypothesized that RPE cell energy metabolism might prioritize the diffusion of glucose to the retina by limiting its consumption.

To compare glucose metabolism in RPE versus in retina, we initially used two preparations, freshly dissected mouse retina (mRetina) and cultured human fetal RPE cells (hfRPE). The hfRPE cells were grown 4-6 weeks in culture to form a monolayer with tight junctions and a trans-epithelial resistance similar to native human RPE (≥200 Ω•cm^2). Due to its similarity to native RPE cells, this hfRPE preparation has been widely used to study RPE metabolism and to model RPE-related diseases such as age-related macular degeneration (Ablonczy et al., 2011; Adijanto and Philp 2014; Blenkinsop et al., 2015; Johnson et al., 2011; Sonoda et al., 2009). We added ^{13}C-labeled glucose to both preparations and then used gas chromatography mass spectrometry(GC-MS) (Du et al., 2015) to compare incorporation of ^{13}C into glycolytic and TCA cycle intermediates. For these experiments we used [1,2] ^{13}C glucose because the pattern of ^{13}C labeling from this isotopomer can be used to distinguish metabolites generated by glycolysis from metabolites generated by the pentose phosphate pathway (Metallo et al., 2009). Metabolites with one ^{13}C (“m1”) are generated from glucose that flows through the oxidative reactions of the pentose phosphate pathway whereas metabolites with two ^{13}C (“m2”) are produced when glucose enters glycolysis directly. In a previous report (see Fig. S2C of (Du et al., 2016b)) we used [1,2] ^{13}C glucose to show that < 2% of metabolic flux from glucose goes through the pentose phosphate pathway in both mRetina and hfRPE.

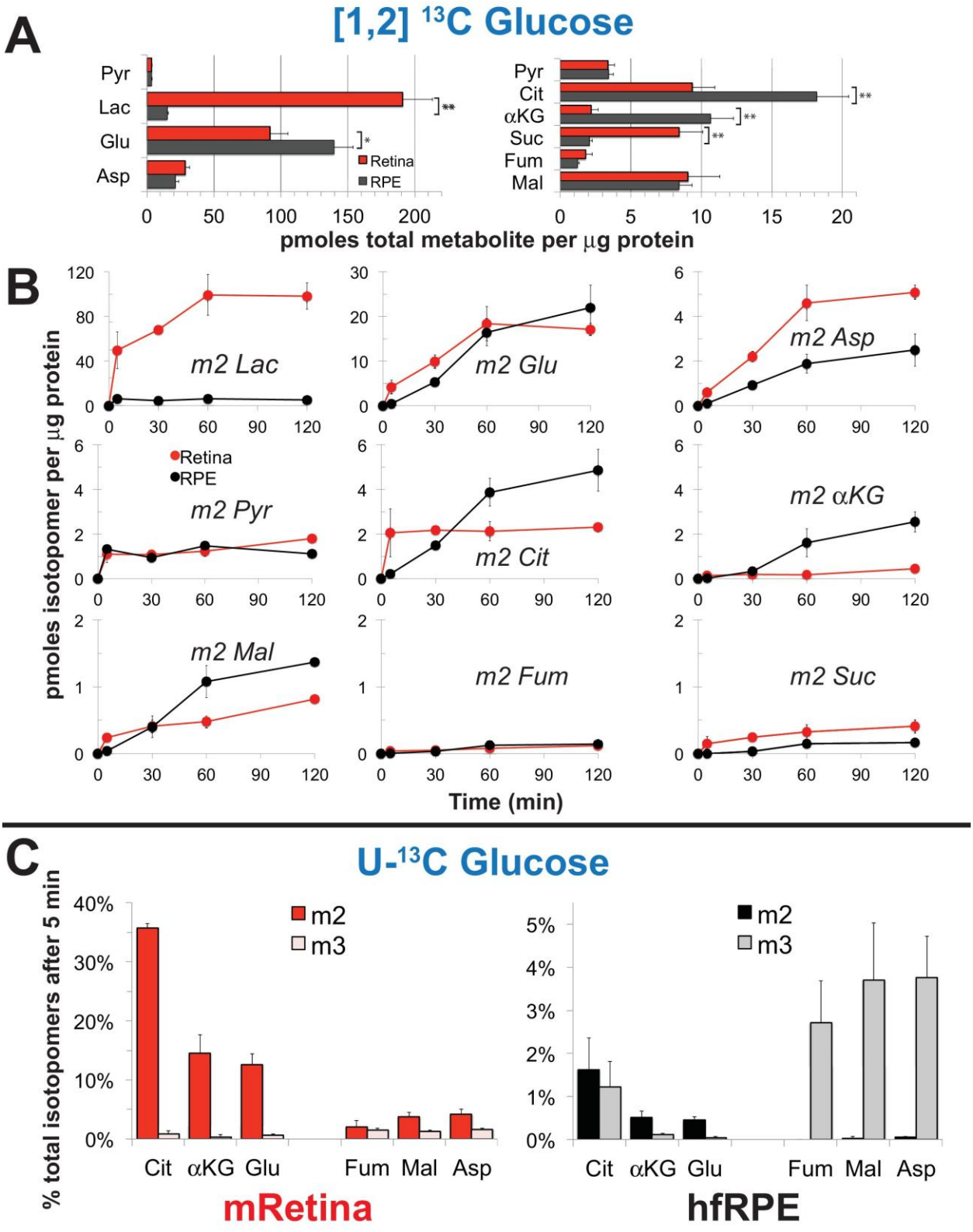

Fig. 2.3. Differences in metabolic flux in retina and RPE. **(A)** Total metabolite levels (pmoles per µg protein) in mRetina (red) and hfRPE (black). (n = 11) Note the different

scales for the left and right panels. * $p < 0.05$ and ** $p < 0.01$. **(B)** Incorporation of ^{13}C from [1,2] ^{13}C glucose into metabolites in mRetina and hfRPE cells (pmoles per µg protein). Each of the isotopomers shown is derived from glucose metabolized by glycolysis. Note the different scales for the top, middle and bottom panels. (n = 3 for each time point; error bars represent standard deviation). **(C)** Incorporation in mRetina and hfRPE cells of ^{13}C from 5 mM U-^{13}C glucose into metabolites after 5 minutes. The % of total isotopomers that are m2 and m3 are shown.

Fig. 2.3A shows the total pmoles per µg protein of several metabolites in mRetina and in hfRPE. There are several striking differences. Lactate and succinate are more abundant in mRetina than in hfRPE, whereas citrate and α-ketoglutarate are more abundant in hfRPE than in mRetina. Fig. 2.3B shows the time course of incorporation of ^{13}C from [1,2] ^{13}C glucose into several key metabolites. The initial rate at which ^{13}C from glucose incorporates into the intracellular pool of lactate is at least 8 times faster in mRetina than in hfRPE. We also noted that the citrate and α-ketoglutarate pools are larger and fill more gradually in hfRPE cells than in retina indicating a large oxidative metabolic capacity of RPE mitochondria. It is important to note that interpretation of metabolic flux in the retina in each of the panels in Fig. 2.3 is complicated by the presence of multiple cell types and multiple compartments within each cell type.

We also incubated mRetina and hfRPE with U-^{13}C glucose because this isotopomer allows us to compare more directly the relative rates of carboxylation and decarboxylation of pyruvate. Mitochondrial intermediates with two labeled carbons (“m2”) are produced by decarboxylation of pyruvate, whereas those with three labeled carbons (“m3”) are made by carboxylation of pyruvate. (Fig. 2.5B shows a schematic of these pathways). Fig. 2.3C shows that decarboxylation of pyruvate predominates in mRetina, whereas carboxylation is more prominent in hfRPE.

The findings in Fig. 2.3 support our hypothesis that retina and RPE cells metabolize glucose differently. In a previous study we showed that RPE cells also use an alternative pathway, reductive carboxylation, to make NADPH (Du et al., 2016a). We propose that these differences are adaptations that give RPE cells the ability to minimize consumption of glucose so that they can maximize transport of glucose from the choroid to the retina.

Confirmation of metabolic specializations of the retina and RPE in a mouse eye. The analyses of RPE metabolism in Fig. 2.3 focused on the cultured hfRPE cell. This is a well characterized model that has been used to evaluate RPE metabolism (Adijanto and Philp 2014). *In vitro* studies have focused on cultured hfRPE cells because RPE cells isolated from adult eyes can de-differentiate in culture. A recent report compared human adult RPE, fetal RPE, and native adult RPE and found some differences in gene expression and trans-epithelial resistance. However, the results indicate that the cultured adult human RPE is not better than hfRPE as a representation of native RPE (Blenkinsop et al., 2015). hfRPE cells also have been used as a cell culture model for studying various diseases, including age-related macular degeneration (Johnson et al., 2011). The hfRPE cultures used in the experiments reported here are of a similar age in culture as the ones used in other published studies, including those used to model AMD.

Nevertheless, it is important to confirm that the metabolic differences between mouse retina and hfRPE in Fig. 2.3 reflect *bona fide* metabolic differences between retina and RPE in an eye. To do that we evaluated metabolic differences between isolated mouse retina and a mouse eyecup (mEC) preparation in which the RPE remained intact after the retina was removed. Although the choroid and sclera also are present in this preparation, the RPE layer is metabolically active and it is the layer most accessible to added metabolites. We incubated the freshly separated retinas and eyecups in medium containing glucose and glutamine and then analyzed metabolites by GC-MS. Fig. 2.4A compares the ratio of total lactate to total citrate in the retina vs. in the eyecup. Similar to the comparison of the lactate/citrate ratio for mouse retina vs. hfRPE, the lactate/citrate ratio in the mouse retina is nearly 30 times higher than in the mouse eyecup.

The data shown in Fig. 2.3 reports the amounts of intracellular metabolites. Some of the ^{13}C-labeled metabolites made from ^{13}C glucose, most notably ^{13}C lactate, could be exported to the medium. To quantify exported metabolites, we incubated retinas, eyecups and hfRPE cells with U-^{13}C glucose and measured accumulation in the medium of ^{13}C labeled lactate and pyruvate (Fig. 2.4B, C). After a ~5 minute delay,

retinas, hfRPE cells and eyecups exported ^{13}C lactate and ^{13}C pyruvate. Retina releases ^{13}C lactate into the medium ~20 times faster than either hfRPE or mEC.

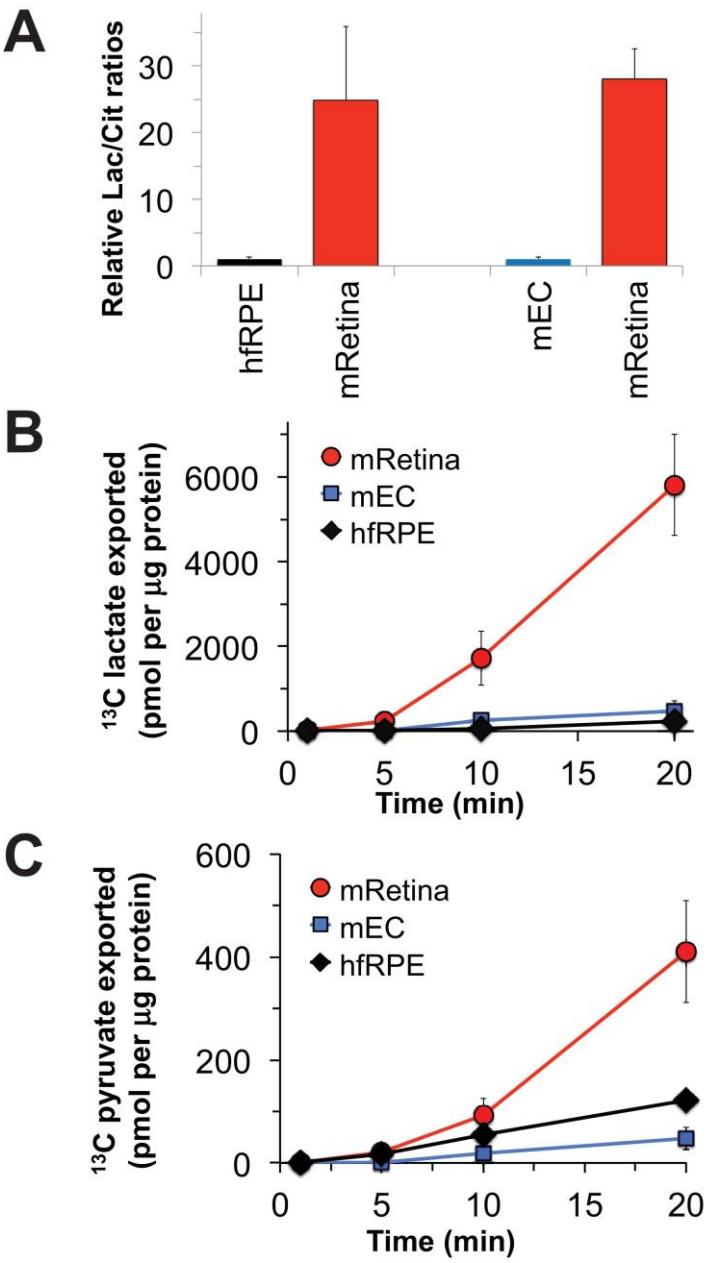

Fig. 2.4. Comparisons of metabolic flux in mouse retina (mRetina), mouse eyecup (mEC), and human fetal RPE (hfRPE). **(A)** Ratios of total intracellular lactate/citrate in both hfRPE and mEC are about 1/25 of the lactate/citrate ratio in mRet. **(B)** Accumulation of m3 ^{13}C lactate in the medium in which either mRetina (n=4), mEC (n=4) or hfRPE (n=3) were incubated with 5 mM U-^{13}C glucose. **(C)** Accumulation of m3 ^{13}C pyruvate in the media in which either mRetina (n=4), mEC (n=4) or hfRPE (n=3) were incubated with 5 mM U-^{13}C glucose. Error bar report standard error of the mean.

RPE cells can use lactate as a fuel.

In previous reports we confirmed that mouse retinas convert most of the glucose they consume into lactate (Du et al., 2016a) and retinas release more lactate than other neuronal tissues (Du et al., 2013a). Figs. 2.3 and 2.4 in this report show that mouse retinas produce and release more lactate than RPE cells. We considered the possibility that the RPE can use lactate exported from a retina as an alternative fuel to minimize consumption of glucose by the RPE. To determine if hfRPE can use lactate, we incubated monolayers of hfRPE cells either with 5 mM U-^{13}C glucose or with 10 mM U-^{13}C lactate/1 mM unlabeled glucose for 5 or 10 minutes. We then quantified incorporation of ^{13}C into glycolytic and TCA cycle metabolites. Fig. 2.5A shows that ^{13}C incorporates rapidly into the pyruvate pool from both ^{13}C glucose and ^{13}C lactate. However, in the citrate pools, ^{13}C from lactate accumulates at least 20 times faster than ^{13}C from glucose. We also noted that substantial amounts of m3 malate form, indicating that carboxylation of pyruvate is a significant metabolic pathway in hfRPE. Fig. 2.5B quantifies the rates of incorporation of ^{13}C from lactate into TCA cycle intermediates in hfRPE cells. To confirm that utilization of lactate is similar in hfRPE and mEC we measured incorporation of ^{13}C from U-^{13}C lactate into metabolic intermediates in hfRPE and compared its incorporation into mRetina and mEC. Fig. 2.6 shows that ^{13}C lactate metabolism in hfRPE is more similar to mEC metabolism than to retina metabolism.

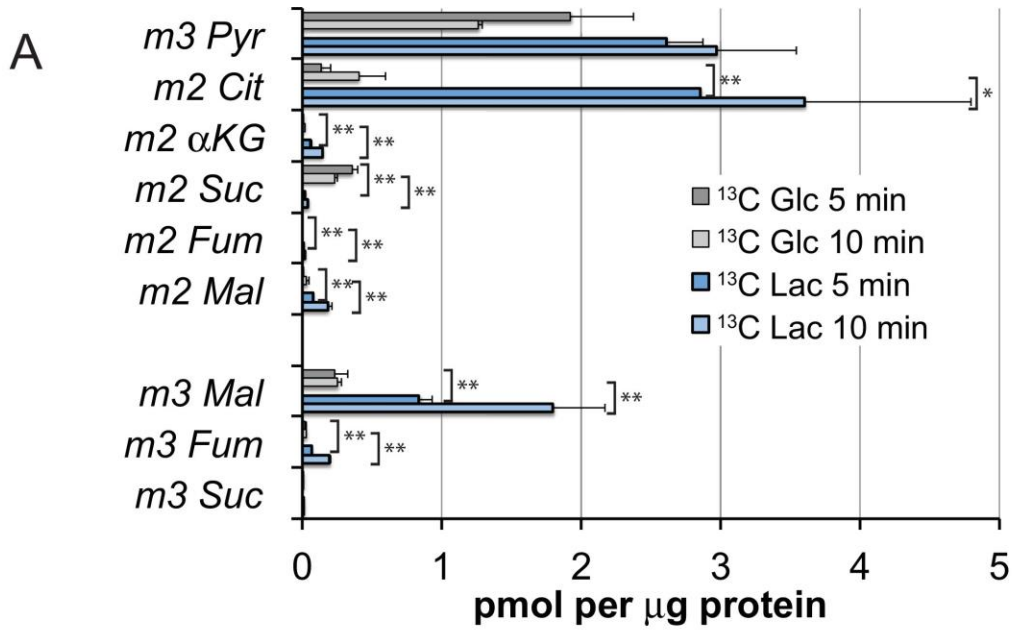

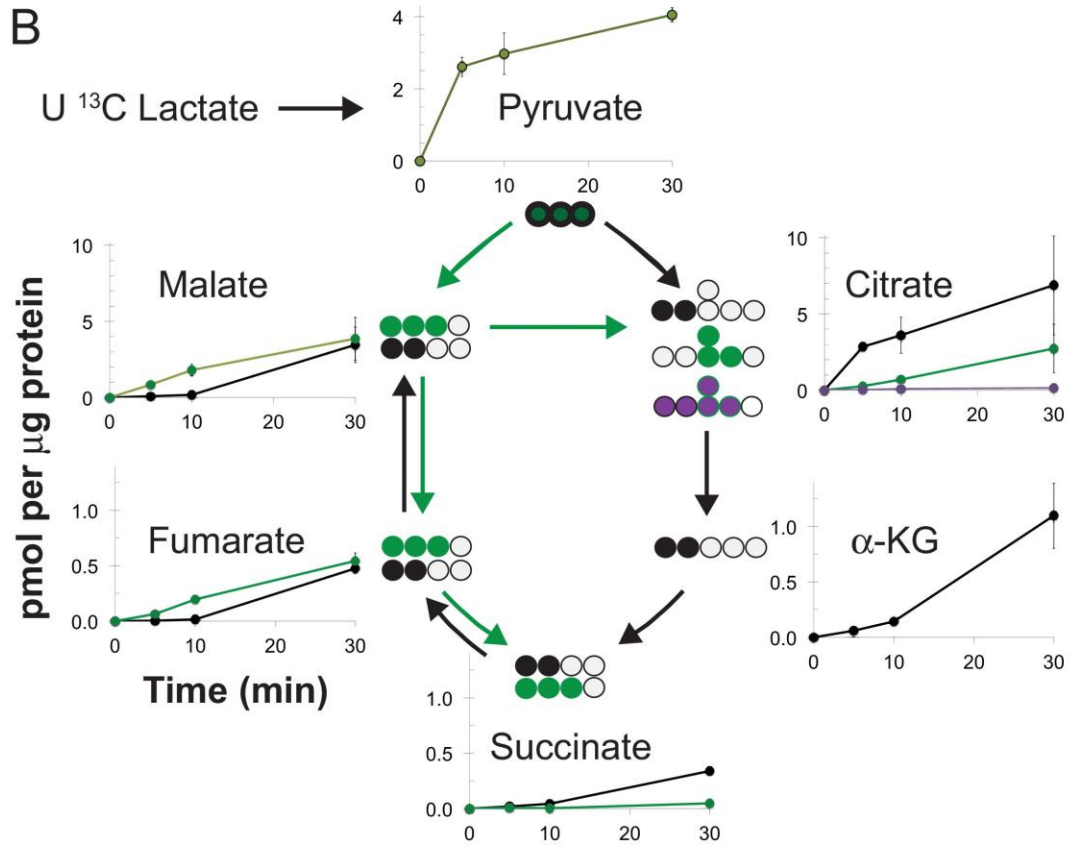

Fig. 2.5. Incorporation of ^{13}C from lactate into metabolic intermediates in hfRPE cells. **(A)** Comparison of initial rates of labeling (at 5 and 10 minutes after introduction of labeled fuel) from 5 mM U-^{13}C glucose vs. from 10 mM U-^{13}C lactate (with 1 mM unlabeled glucose also present). Citrate and malate take up label faster from lactate than from glucose. **(B)** Time courses of incorporation of ^{13}C from 10 mM U-^{13}C lactate

(with 1 mM unlabeled glucose also present) into hfRPE metabolites accompanied by schematic illustrations of the labeled species in the context of the TCA cycle. (n = 2-3 for each time point; error bars represent range or standard deviation).

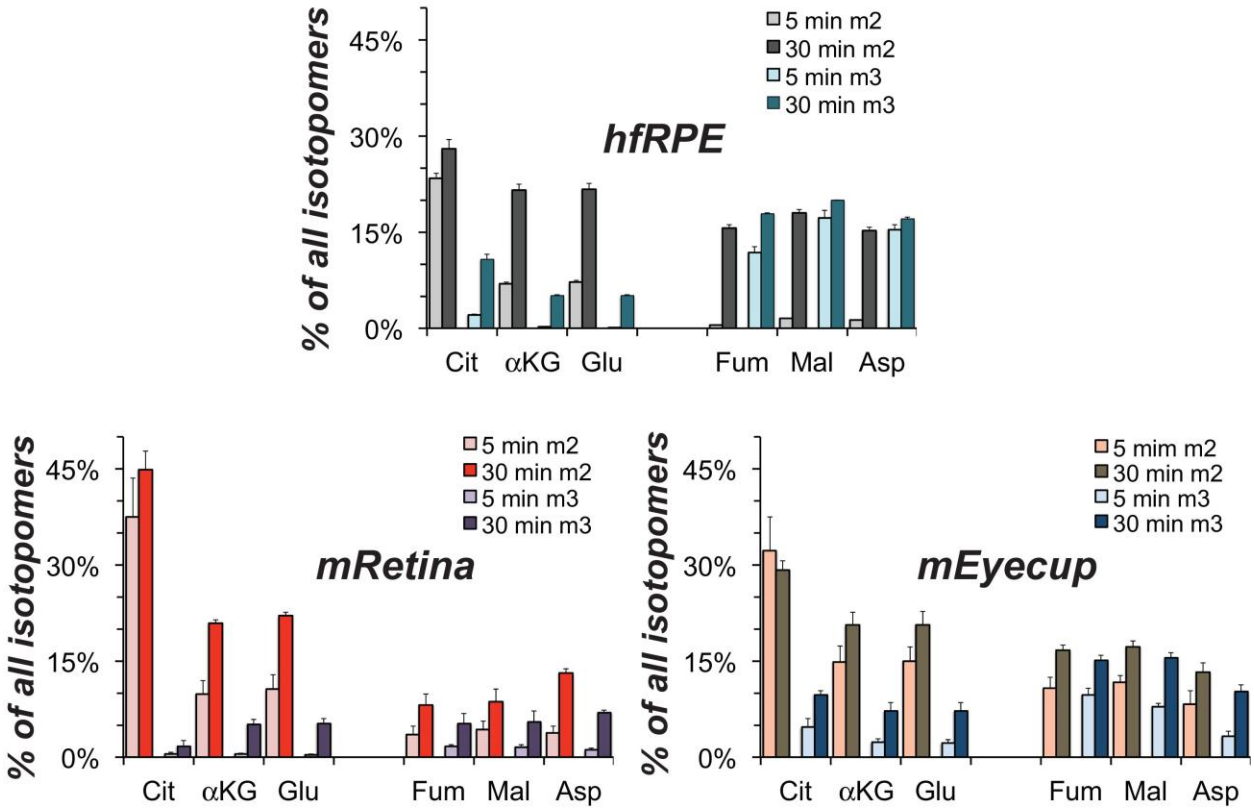

Fig. 2.6. Comparison of lactate metabolism in hfRPE with lactate metabolism in mouse retina and mouse eyecups with retinas removed. The high relative abundance of m3 metabolites derived from carboxylation reactions and the high abundance of fumarate, malate and aspartate in hfRPE cells resemble the metabolite distributions in the RPE enriched eyecup more than the distributions in retina. Each preparation was incubated with 10 mM U-^{13}C lactate for the specified times and metabolites were extracted, derivatized and quantified by GC-MS. (n=2 for hfRPE, n= 3 for mEyecup and n=4 for mRetina; error bars represent range of standard deviations.).

Lactate can suppress glucose catabolism in RPE cells.

Fig. 2.5 and 2.6 show that RPE cells can consume lactate as an alternative to using glucose for fuel. We next asked whether lactate also can suppress consumption of glucose. We hypothesized (Fig. 2.7A) that lactate dehydrogenase (LDH) in RPE cells can use lactate to reduce cytosolic NAD^+ to NADH as it does in other cells (Hung et al., 2011). Since NAD^+ is required for glycolysis, depletion of NAD^+ by lactate and LDH could suppress glycolysis so that RPE cells would consume less glucose.

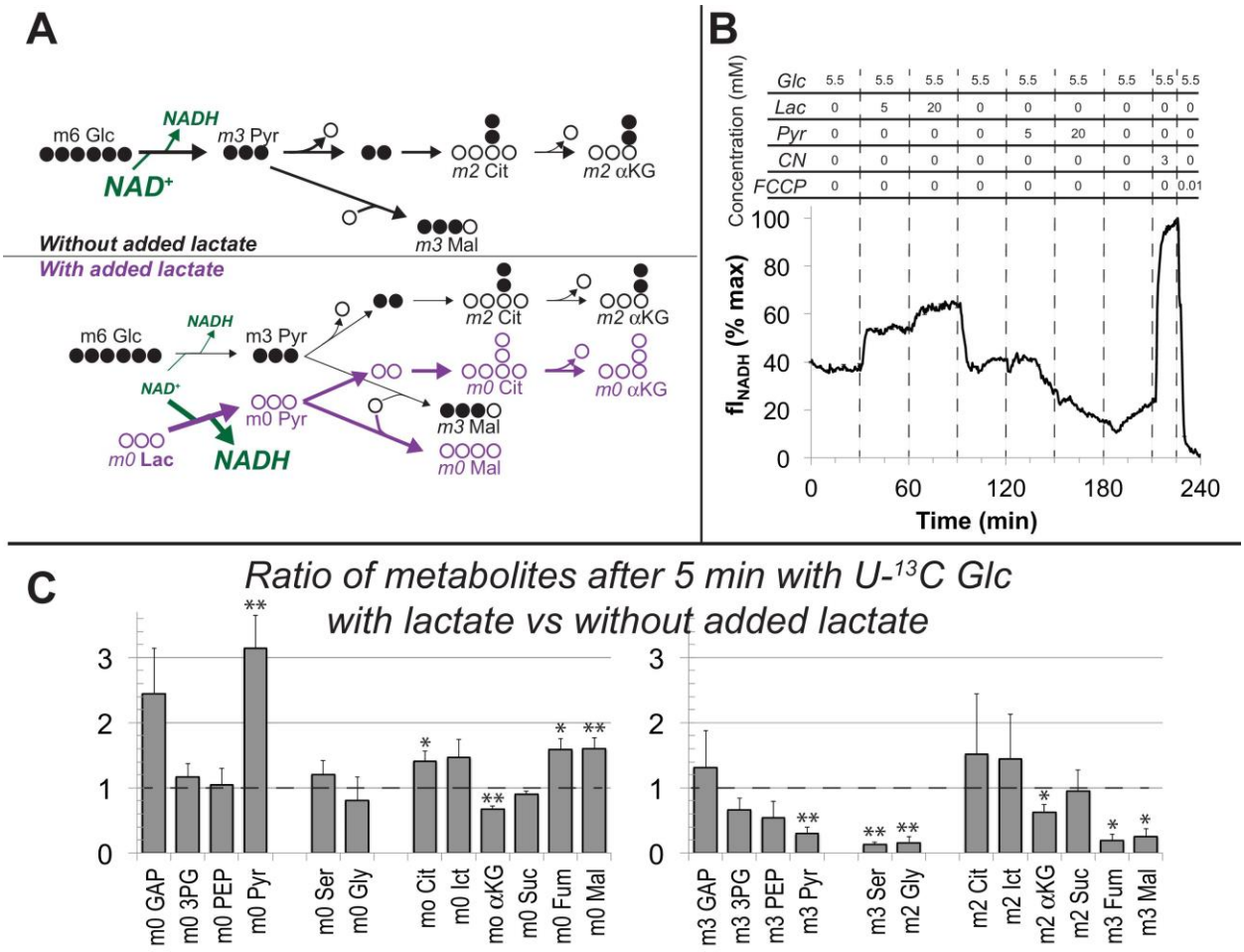

Fig. 2.7. Lactate suppresses oxidation of glucose by hfRPE cells. **(A)** Schematic prediction of how U-^{13}C Glc ("m6 Glc") would be metabolized without lactate (top) vs. with lactate (bottom). We hypothesized that lactate would suppress glycolysis of m6 Glc by depleting NAD$^+$. The model also predicts that unlabeled (m0) pyruvate and TCA cycle intermediates become more abundant. **(B)** Effect of lactate and pyruvate on total cellular NADH measured by fluorescence in a monolayer of hfRPE cells as described in methods. The graph shows the average from 3 individual cells and is representative of 3 similar experiments. **(C)** Ratios of metabolites after 5 min with U-^{13}C Glc with lactate (20 mM) vs. without added lactate. Lactate substantially increases the total amounts of unlabeled (m0) GAP, pyruvate, citrate, isocitrate, fumarate and malate (left panel) in hfRPE cells. The right panel shows that lactate suppresses the incorporation of ^{13}C from 5 mM ^{13}C Glc into glycolytic and TCA intermediates. (n = 3; error bars represent SE, * indicates $p < 0.05$ and ** indicates $p < 0.01$ for the comparison of with vs. without added unlabeled lactate.

We tested the hypothesis that bathing hfRPE cells in lactate converts their NAD$^+$ into NADH. We used a perfusion apparatus with an inverted microscope to measure total NADH fluorescence (Santos et al., 2017) from hfRPE monolayers (Fig. 2.7B). The cells

first were equilibrated with media containing 5.5 mM glucose. The perfusion solution then was changed to 5.5 mM glucose + 5 mM lactate and then to 5.5. mM glucose + 20 mM lactate. After returning the cells to 5.5 mM glucose we then perfused them with 5.5 mM glucose containing 5 mM and then 20 mM pyruvate. Finally, we added cyanide to trap all of the NAD in its reduced state and then FCCP without cyanide to trap all the NAD in its oxidized state. Fig. 2.7B shows that lactate in the medium substantially increases NADH fluorescence, whereas pyruvate drives it to its oxidized state. These results confirm that lactate in the environment of RPE cells can deplete NAD^+ by reducing it to NADH.

To determine if glycolysis in hfRPE is suppressed by lactate-induced depletion of NAD^+ we incubated hfRPE cell monolayers with 5 mM U-^{13}C glucose either in the absence or presence of 20 mM unlabeled lactate. We used this concentration based on a previous measurement of retina and RPE (Kolko et al., 2016; Matschinsky et al., 1968) and because the RPE in an eye must be exposed to high levels of lactate from aerobic glycolysis in the retina. We harvested the cells and used GC-MS to determine if lactate suppresses incorporation of ^{13}C from glucose into glycolysis and the TCA cycle. Fig. 2.7C shows that unlabeled lactate increases unlabeled pyruvate, citrate, isocitrate, fumarate and malate (left panel). This is consistent with the results in Fig. 2.5 showing that carbons from lactate are incorporated rapidly into TCA cycle metabolites through both carboxylation and decarboxylation of pyruvate.

Addition of unlabeled lactate also causes accumulation of glyceraldehyde-3-phosphate (GAP), the triose phosphate immediately upstream of the glyceraldehyde-3-phosphate dehydrogenase (GAPDH) reaction, a reaction that requires NAD^+. Consistent with suppression of GAPDH activity, lactate diminishes incorporation of ^{13}C from U-^{13}C glucose into intermediates downstream of the GAPDH reaction (right panel of Fig. 2.7C). Lactate does not diminish incorporation of ^{13}C from glucose into m2 citrate and m2 isocitrate. This may reflect enhanced TCA cycle activity caused by anaplerotic supplementation of unlabeled TCA cycle intermediates (see left panel of Fig. 2.7C). We conclude that exogenous lactate can suppress glycolysis in hfRPE cells.

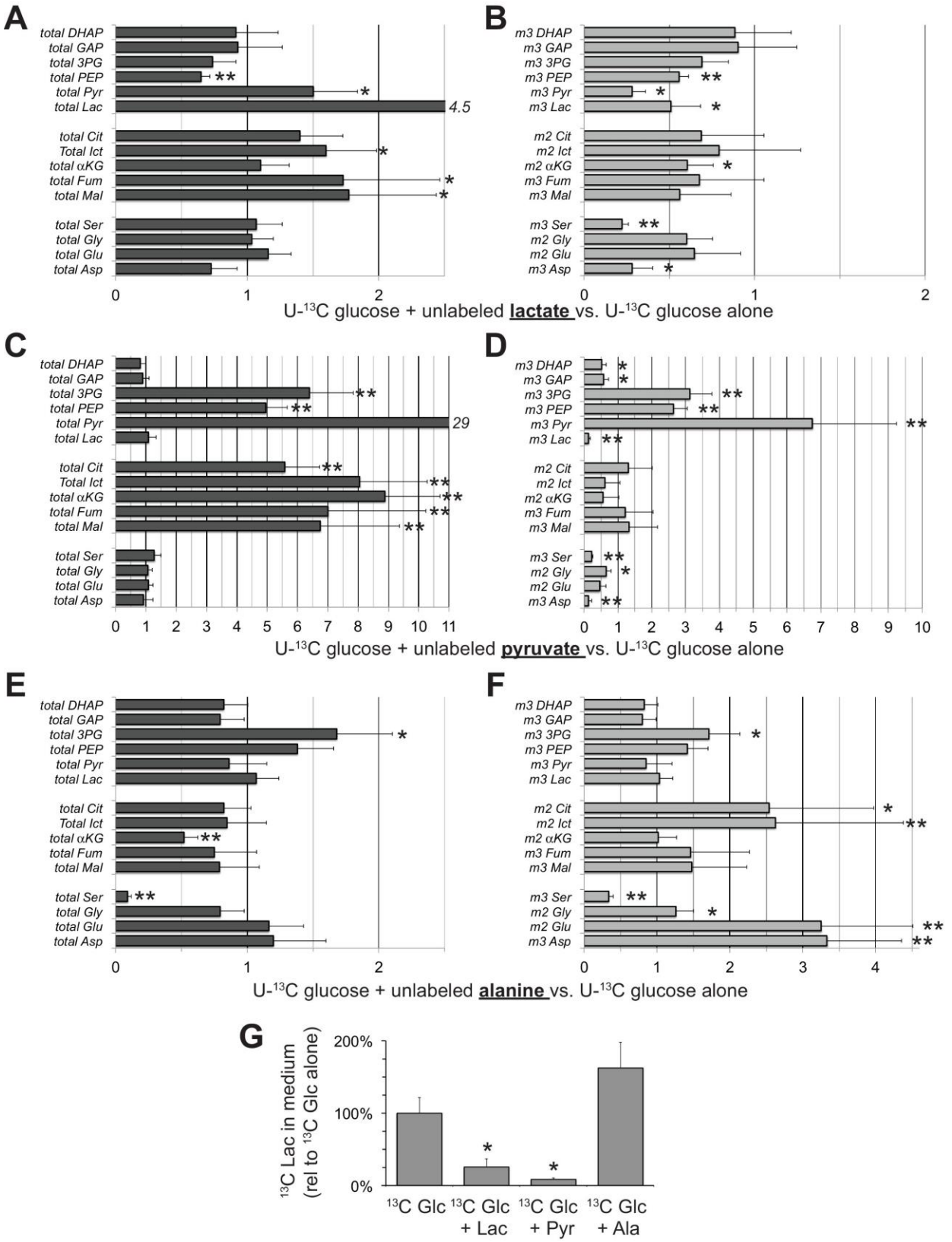

Fig. 2.8. Effects of lactate, pyruvate and alanine on metabolic flux from U-^{13}C glucose in hfRPE cells. Each bar graph compares the ratio of metabolites with vs. without the

addition of 10mM of either unlabeled lactate **(A, B)** pyruvate **(C, D)** or alanine **(E, F)**. **A**, **C**, and **E** report the ratios for the total of all isotopomers of each metabolite and **B**, **D** and **F** report the ratios for specific labeled metabolites (m2 or m3). Panel **G** shows the effects of adding unlabeled lactate, pyruvate or alanine on the release of ^{13}C lactate generated by glycolysis of U-^{13}C glucose. Metabolites were extracted, derivatized and quantified after 5min incubation wit 5mM U-^{13}C glucose (n=3) or 5mM U-^{13}C glucose plus 10mM unlabeled lactate (n=3), pyruvate (n=3) or alanine (n=3). Error bars report StDev. *p<0.05; **p<0.01.

Lactate at a concentration of 20 mM may seem non-physiological because it is higher than the concentration typically found in serum. We also tested the effect of 10 mM lactate and found similar suppression of glycolysis, i.e. suppression of the formation of m3, but not m0 glycolytic intermediates (Fig. 2.8A,B). We also measured the effect of pyruvate, which drives NAD to its oxidized state as can be seen from Fig. 2.7B. Pyruvate and its amino acid derivative, alanine, *cause* redistributions of the relative amounts of specific glycolytic and mitochondrial intermediates, (Fig. 2.8C-F). The effect of pyruvate may be attributable to accumulation of cytosolic NAD^+ accelerating GAPDH activity while at the same time inhibiting malate-aspartate shuttle activity (Du et al., 2013a). Alanine raises the levels of glutamate and aspartate, which may counteract the effect of pyruvate, derived from the alanine, on the malate-aspartate shuttle. SLC25A11 AND SLC25A13 transcripts, which encode the mitochondrial transporters required for malate-aspartate shuttle activity, are present in RPE/choroid preparations (Whitmore et al., 2014). Fig. 2.8G shows that both lactate and pyruvate suppress accumulation of ^{13}C lactate in the medium whereas alanine enhances it.

Lactate can enhance transport of glucose across a monolayer of hfRPE cells.

We hypothesized that lactate can enhance the net flow of glucose across the RPE because lactate can suppress glycolysis. The simplest version of this hypothesis is that the suppression of glycolysis by lactate (as shown in Figs 2.7 and 2.8) minimizes consumption of glucose, so that more glucose can diffuse successfully from the basolateral to the apical side of the RPE.

To test this hypothesis, we measured the influence of lactate on transport of glucose across a monolayer of hfRPE cells. We grew hfRPE cells on transwell filters to confluence with a transepithelial resistance ≥200 Ω•cm^2. We added either 2 mM or 5 mM ^{13}C glucose (^{13}C Glc) to the chamber on the basolateral side, the side of RPE cells that normally faces the choroidal blood supply in an eye. We then used liquid chromatography mass spectrometry to quantify accumulation of ^{13}C glucose in chamber on the apical side, where RPE cells normally would face a lactate-rich retina. We performed this experiment either with no added lactate or with unlabeled lactate added to medium on the apical side (Fig. 2.9A). First, we measured the effects of adding unlabeled lactate, pyruvate or alanine to the apical side to determine if they affect the initial rate at which basolateral ^{13}C Glc reaches the apical side of the hfRPE monolayer in this experimental configuration (Fig. 2.9B). None of the additions had more than a minor influence on this initial rate. We also quantified the effects of these additions on the production and release of ^{13}C pyruvate (^{13}C Pyr) (Fig. 2.9C) and ^{13}C Lactate (^{13}C Lac) (Fig. 2.9D) in the apical chamber. Unlabeled pyruvate had the most pronounced effect, substantially inhibiting the accumulation of labeled pyruvate and lactate in the apical chamber.

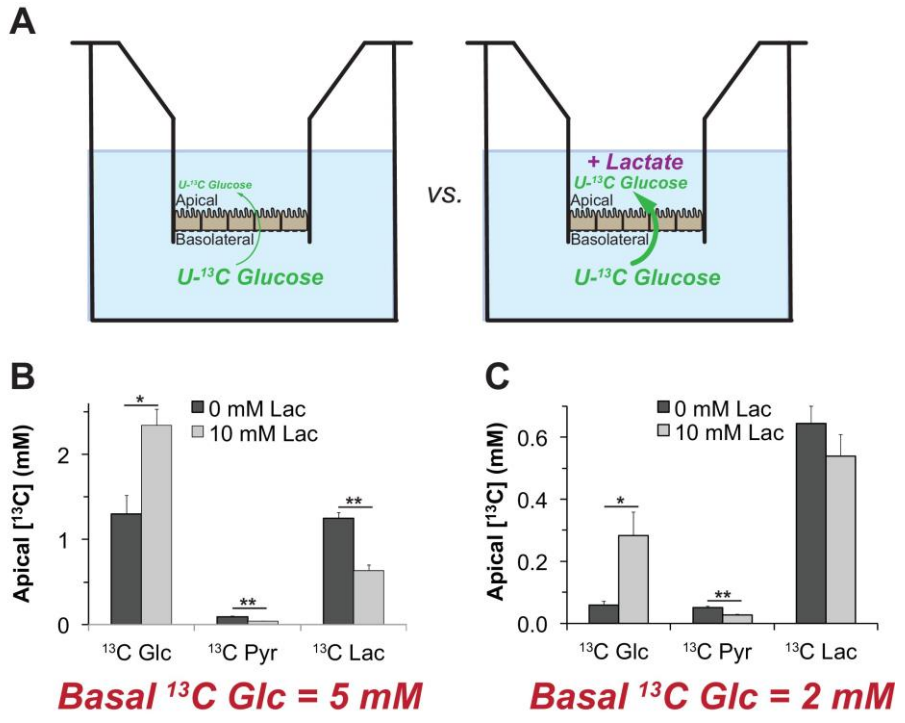

Fig. 2.9. Lactate can enhance transport of glucose across a monolayer of RPE cells. **(A)** Strategy to evaluate the effect of lactate on transport of glucose across a monolayer of RPE cells. We hypothesized that without lactate (left) glycolysis consumes glucose before it can cross the RPE cell monolayer. With lactate on the apical side (right) glycolysis would be partially suppressed so more glucose can cross the monolayer without being consumed by glycolysis. **(B, C)** Glucose

on the apical side after 8hr. These panels compare the concentrations of, ^{13}C Pry, and ^{13}C Lac in the apical chamber 8hr after 5mM **(B)** or 2mM **(C)** ^{13}C Glc was added to the basolateral chamber (n=3).

We also quantified the effect of 10 mM unlabeled lactate on accumulation of ^{13}C Glc in the apical chamber after a longer, 8 hour, incubation (Fig. 2.9E,F). We focused this experiment on lactate because it is most physiologically relevant. In separate experiments with mouse retinas we found that pyruvate is released from mouse retinas at only 6.7 ± 2.3% of the rate of lactate release and alanine is released at only 0.4% ± 0.1% of that rate (StDev, n = 13). This longer time course showed that unlabeled lactate added to the apical medium substantially increases the accumulation of ^{13}C glucose on the apical side (Fig. 2.9E,F). The effect of lactate is more pronounced when 2 mM ^{13}C Glc (Panel F) instead of 5 mM ^{13}C Glc (Panel E) is used, consistent with lactate suppressing consumption of glucose by the RPE.

Unlabeled lactate in the apical compartment also suppresses accumulation of ^{13}C Pyr and ^{13}C Lac on the apical side (Fig. 2.9E,F). These findings are consistent with our hypothesis that high concentrations of lactate released from a retina at the apical side of the RPE can protect glucose so that more of it reaches the retina.

DISCUSSION

Model for a network of metabolic interdependence between the retina and RPE.

Fig. 2.10 summarizes our model for the retina-RPE metabolic ecosystem. We propose that lactate from photoreceptors suppresses glycolysis in the RPE so more glucose can reach the retina.

Previous evidence that cells in the retina have specific metabolic roles.

The distributions of metabolic enzymes in mouse retina indicate that photoreceptors have the enzymes and transporters they need for glycolysis, but MGCs do not. Glycolysis requires pyruvate kinase (PK). The M2 isoform of PK (PKM2) is highly enriched in photoreceptors (Lindsay et al., 2014; Chinchore et al., 2017; Rajala et al., 2016; Rueda et al., 2016; Casson et al., 2016) but MGCs in mouse retinas do not

express substantial amounts of any PK isoform (Lindsay et al., 2014). MGCs also do not express hexokinase (Rueda et al., 2016). Furthermore, lactate, rather than glucose, is the most effective source (Lindsay et al., 2014) of carbon for glutamine synthesis by MGCs (Riepe and Norenburg 1977) in mouse retinas. Based on these observations, we proposed that MGCs in a retina are fueled by lactate from photoreceptors (Hurley et al., 2015). Based on those findings and the results described in this report, we propose that the central role of photoreceptors in retinal energy metabolism is to convert glucose to lactate, which then is used as fuel by both RPE and MGCs (Fig. 2.10).

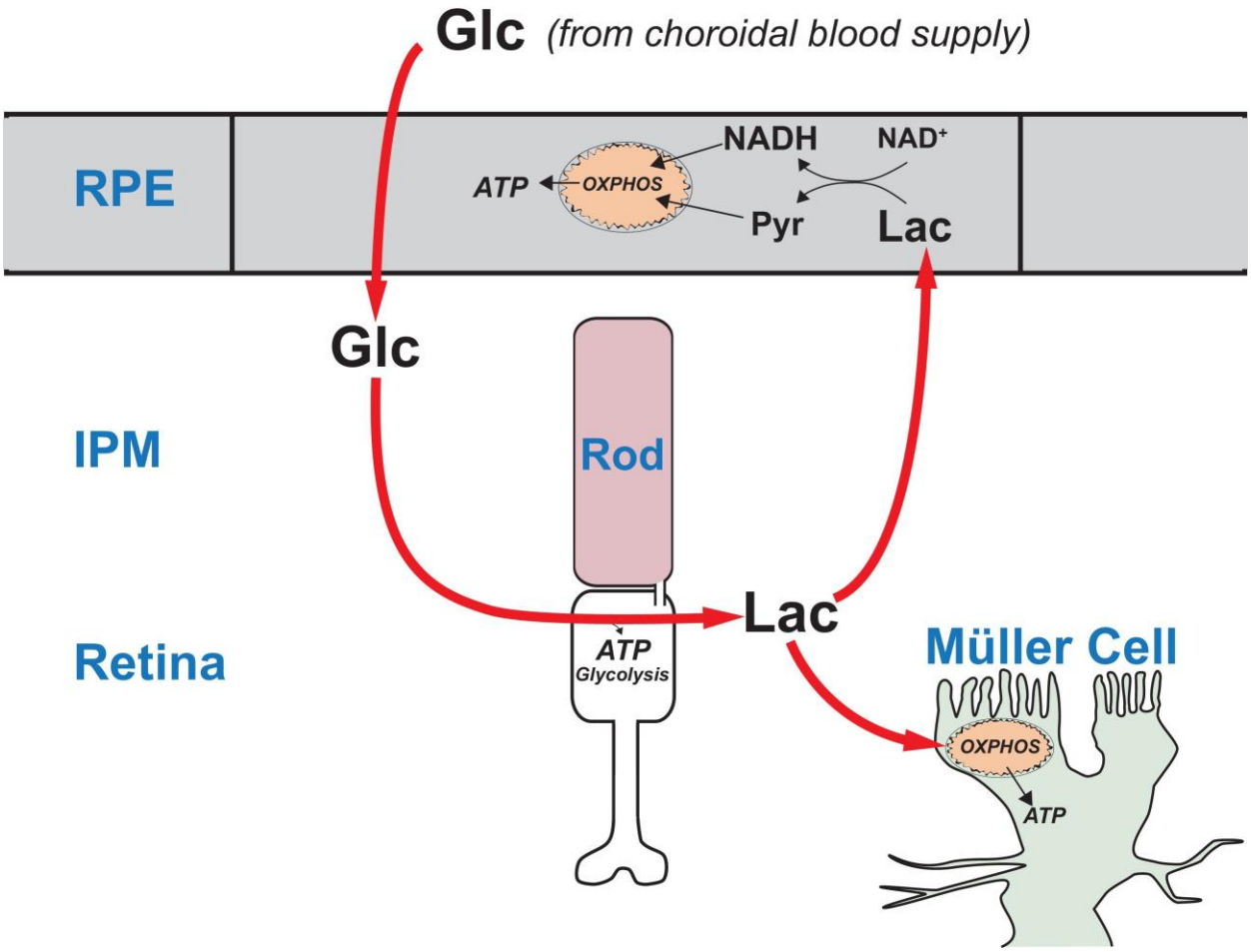

Fig. 2.10. A working model that describes the flow of metabolic energy in the retina-RPE ecosystem. Photoreceptors convert glucose into lactate and release the lactate into the interphotoreceptor matrix. Lactate suppresses glycolysis in RPE cells by depleting NAD^+. Lactate also fuels metabolic activity in Müller cells, which lack key enzymes that would be required for glycolysis.

Significance of aerobic glycolysis in the retina.

Enhanced capacity for anabolic metabolism has been proposed as the purpose of aerobic glycolysis in photoreceptors (Lindsay et al., 2014; Chinchore et al., 2017; Rajala et al., 2016), but our model suggests an additional purpose. We propose that the laminated structure of the eye, in which the RPE separates the retina from its source of nutrients, requires photoreceptors to produce and release lactate to suppress glycolysis so that sufficient glucose can flow through the RPE.

The "retinal ecosystem" model helps explain *in vivo* findings from genetically altered photoreceptors and RPE.

The *in vitro* experiments in Figs. 2.7 and 2.8 identify the metabolic effects on glucose consumption of adding additional fuels like lactate, pyruvate and alanine. The *in vitro* experiments in Fig. 2.9E and F show that lactate can protect glucose from consumption by RPE cells. However, more direct evidence will be needed to test whether the model in Fig. 2.10 accurately describes the metabolic relationships in the eye of a living animal. Genetic manipulations of photoreceptor and RPE cells and *in vivo* analyses of their phenotypes are needed. In fact, recent genetic studies do support the model in Fig. 2.10. Photoreceptors engineered to be more glycolytic are more robust than normal and RPE cells engineered to be more glycolytic cause photoreceptors to degenerate (Zhang et al., 2016; Venkatesh et al., 2015; Kurihara et al., 2016; Zhao et al., 2011). According to our model (Fig. 2.10) when photoreceptors are made to be more glycolytic than normal they produce more lactate, which more effectively suppresses glycolysis in the RPE. More glucose reaches the retina and photoreceptor survival is enhanced. When RPE cells are engineered to be more glycolytic they consume more glucose, leaving less glucose available for the retina. Photoreceptors become starved, stressed, and degenerate.

The concept of a metabolic ecosystem and its relationship to retinal disease.

The "retina ecosystem" model in Fig. 2.10 suggests an explanation for the linkage between Age-Related Macular Degeneration and accumulation of mitochondrial DNA damage in RPE cells (Terluk et al., 2015). Photoreceptors may starve when RPE

mitochondria fail because the RPE becomes more dependent on glycolysis, which prevents glucose from reaching the retina.

The concept of a metabolic ecosystem also has implications for other types of retinal disease. Mutations that affect genes expressed only in rods can cause rods to degenerate. However, cones subsequently degenerate as a consequence of the loss of rods, even though the cones are not affected directly by the mutant gene (Punzo et al., 2012). One reason for this is that loss of a cone viability factor that normally is produced by rods may contribute to cone degeneration in this type of diseased state (Ait-Ali et al., 2015). The model in Fig. 2.10 suggests another factor that also can contribute to the secondary loss of cones when rods degenerate. A retina without rods makes less lactate (Du et al., 2016a). We have shown in this report that, without lactate to suppress glycolysis, RPE cells oxidize more glucose. This may explain why rods and cones that are genetically normal are shorter and dysmorphic when they are in an environment where most of the surrounding photoreceptors have degenerated (Koch et al., 2017; Lewis et al., 2010). The loss of lactate production in rod-deficient retinas may limit the rate at which glucose can reach cones. This is consistent with starvation of cones (Punzo et al., 2009) and accumulation of 2-NBDG in RPE cells (Wang et al., 2016) when rods degenerate. Also in support of the model in Fig. 2.10, an alternative supply of glucose can rescue those cones from degeneration (Wang et al., 2016).

Other fuels also have important roles in the metabolic ecosystem.

This study highlights one way that RPE, photoreceptors, and MGCs can work together as an ecosystem of metabolically specialized and interdependent cells. Our investigation focused primarily on lactate because the retina produces copious amounts of it, but glycogen (Senanayake et al., 2006), fatty acids (Joyal et al., 2016; Reyes-Reveles et al., 2017), ketone bodies (Adijanto et al., 2014), glutamine (Du et al., 2016b), proline (Chao et al., 2017) and metabolites from other metabolic pathways (Rueda et al., 2016; Chao et al., 2017) also must contribute significantly to this metabolic ecosystem. RPE cells accumulate and breakdown glycogen (Senanayake et al., 2006) so it is likely that glycogen in RPE cells is a glucose buffer that acts either directly in the glucose

transport pathway or in an alternative pathway. Future experiments exploiting the availability of ^{12}C and ^{13}C isotopomers of glucose may allow investigators to define the role of glycogen in glucose transport across RPE cells. One recent study showed that oxidation of fatty acids by the RPE can supply the retina with ketone bodies (Adijanto et al., 2014) and another showed that RPE can oxidize fatty acids from photoreceptor phagocytosis, (Reyes-Reveles 2017). Like lactate, fatty acids also may be able to suppress consumption of glucose by the RPE. Future investigations will be necessary to confirm this. Altogether, these studies suggest that energy homeostasis in retina and RPE relies on a complex and specialized metabolic interplay between metabolically distinct cells in the retina and RPE. A better understanding of this metabolic ecosystem could be used to develop therapies for a range of retinal degenerative diseases.

MATERIAL AND METHODS

Animals.

All research was authorized by the University of Washington Institutional Animal Care and Use Committee. Mice in the C57BL6J background were maintained in the University of Washington South Lake Union vivarium at 27.5 ºC on a 14h/10h light-dark cycle. C57BL/6J does not carry the rd8 mutation in the Crb1 gene (Mattapallil et al., 2012). Transgenic mice expressing eGFP under the Nrl promoter (Akimoto et al., 2006) (RRID:IMSR_JAX:021232), or tdTomato under the Rlbp-CRE promoter (Wohl and Reh 2016) were described previously.

Transgenic heterozygote zebrafish in the AB background were maintained in the University of Washington South Lake Union aquatics facility at 27.5 ºC on a 14h/10h light-dark cycle. Fish used for experiments were male and female siblings between 12-24 months old. A transgenic line stably expressing tdTomato in Müller cells (GFAP:tdTomato; RRID:ZDB-FISH-150901-17843) was described previously (Shin et al., 2014). Prior to gavage experiments, fish were fasted >18 h and dark-adapted >12 h.

Antibodies.

Arrestin1, D9F2 (from Larry Donoso and Cheryl Craft)
IHC: 1:200
GLUT1, (AbCam, ab115730; RRID:AB_10903230)

IB: 1:200,000, 0.86 ng/ml;
IHC 1:1000, 0.17 µg/ml
GLUT3, (AbCam, ab41525; RRID:AB_732609)
IB: 1:5000, 0.136 µg/ml
GLUT4, (AbCam, ab654; RRID:AB_305554)
IB: 1:5000
Glutamine synthetase, (Millipore, MAB302; RRID:AB_2110656)
IHC: 1:1000
MTCO1 (Abcam, ab14705; RRID:AB_2084810)
IHC: 1:2000

Tissue preparations for immunoblotting.

Frozen tissue samples were homogenized in RIPA buffer (150 mM NaCl, 1% Triton X-100, 0.05% sodium deoxycholate, 0.1% SDS, 50 mM Tris, pH 8.0 with a mixed phosphatase and protease inhibitor cocktail (ThermoFisher 88668), briefly sonicated, then rocked at 4°C for 30min. Samples were then spun at 13,300 RPM at 4°C for 15 min, and the supernatant was normalized for loading by BCA assay to 20 µg/tissue. RPE protein lysate was prepared according to a described protocol (Wei et al., 2016). To prepare membrane fractions, frozen tissue samples were homogenized in PBS (0.14 M, pH 7.4) with a mixed phosphatase/protease inhibitor cocktail, then rocked at 4°C for 30 min. Samples were then spun at 45,000 rpm at 4°C, the supernatant (cytosolic fraction) drawn off and saved, and the pellet (membrane fraction) was resuspended in an equal volume of PBS. After mixing with 5X Laemmli loading buffer, 1 µl benzonase (Millipore 70746) was added. Each tissue was then loaded with equal volumes of cytosolic and membrane fraction.

Immunoblotting.

Samples were run on 12%, self-cast acrylamide gels and transferred onto PVDF membranes (Millipore IPFL00010). Following protein transfer, membranes were blocked with LI-COR Odyssey Blocking Buffer (LI-COR, 927-40000) for 1 h at room temperature. Primary antibodies were diluted in blocking buffer and incubated overnight at 4°C. Membranes were washed, incubated with secondary antibody (LI-COR IRDye 800CW, 926-32210, (RRID:AB_621842), and 926-32211, (RRID:AB_621843),1:5000 1h at room

temperature, and washed again. Imaging was performed using the LI-COR Odyssey CLx Imaging System (RRID:SCR_014579).

Immunohistochemistry.

Retinal eyecups were micro-dissected from C57BL6J mice and were fixed in 4% paraformaldehyde in PBS, rinsed with PBS, incubated in a sucrose gradient (5%, 10%, and 20%), embedded into OCT and cryosectioned at 20µm. Mouse sections were washed in PBS, then blocked in IHC buffer (5% normal donkey serum diluted in PBS with 2 mg/mL BSA and 0.3% Triton X-100) for 1 h. Primary antibodies were diluted in IHC blocking buffer as specified, and applied to blocked cryosections overnight at 4°C. Secondary antibodies were diluted at 1:3000 in IHC blocking buffer, and applied to mouse retina sections for 1 h in darkness. Sections were washed in PBS three times, and mounted with SouthernBiotech Fluoromount-G (Fisher Scientific) under glass coverslips and visualized using a Leica SP8 confocal microscope with a 63X oil objective. Images were acquired at a 4096x4096 pixel resolution with a 12-bit depth using Leica LAS-X software (RRID:SCR 013673).

RPE cell culture.

Human fetal eyes with a gestational age of 16-20 weeks were harvested and shipped overnight on ice in RPMI media containing antibiotics from Advanced Bioscience Resources Inc. (Alameda, CA). Dissections of fetal tissue were performed within 24 hours of procurement and followed a modified version of the dissection protocol in order to isolate the retinal pigment epithelium (RPE) (Sonoda et al., 2009). The fetal RPE sheets were incubated at 37°C with 5% CO_2 and cultured in RPE media. The RPE media consisted of Minimum Essential Medium alpha (Life Technologies) supplemented with 5% (vol/vol) fetal bovine serum (Atlanta Biologicals), N1-Supplement (Sigma-Aldrich), Nonessential Amino Acids (Gibco), and a Penicillin-Streptomycin solution (Gibco). Isolated fetal RPE reached confluency about 3-4 weeks after dissection and was then passaged using a 0.25% Trypsin-EDTA solution (Gibco) and passed through a 40 µm nylon cell strainer (BD Falcon) in order to collect a suspension of single cells. After counting, the RPE cells were plated onto 0.3 cm^2 cell culture inserts (Falcon)

coated with Matrigel (Corning) at a seeding density of 100,000 cells per insert. Cells grown on these inserts were cultured in RPE media containing 1% (vol/vol) FBS. Transepithelial resistance was measured weekly after 2 weeks in culture using a Millicell ERS-2 Epithelial Volt-Ohm Meter (Millipore).

Oral Gavage.

Mice were fasted overnight in the dark, and gavaged the next morning in ambient light. A micro-syringe fitted with a 22 gauge 1.5" straight 1.25 mm ball-tip needle was used to orally administer 100 µl of 50 mM 2-NBDG (Invitrogen) dissolved in water. Successfully gavaged mice were returned to darkness during the 2-NBDG incubation period. Zebrafish were gavaged using methods described previously (Collymore et al., 2013) under red light. Briefly, overnight fasted adult zebrafish were anaesthetized > 1 min with 150 mg/mL MS-222 in fish water. Fish were placed in a slit cut in a cellulose sponge soaked with MS-222 solution, and the sponge was rotated to orient the fish mouth up. A micro-syringe fitted with thin, flexible 1 mm OD plastic tubing was used to orally administer 5 µL of either fish water or 30 mM 2-NBDG (Invitrogen). Gavaged fish were immediately placed into a recovery tank of fresh fish water and monitored briefly using a UV flashlight for regurgitation of 2-NBDG. Successfully gavaged fish were returned to darkness during the 2-NBDG incubation period.

Tissue slicing and imaging.

Gavaged mice were euthanized by asphyxiation with CO_2. Zebrafish were euthanized in an ice bath followed by cervical dislocation. Euthanized animals were enucleated, and the retinas dissected away under red light into cold Ringer's solution (133 mM NaCl, 2.5 mM KCl, 1.5 mM NaH_2PO_4, 2 mM $CaCl_2$, 1.5 mM $MgCl_2$, 10 mM HEPES, 10 mM D-glucose, 1 mM sodium lactate, 0.5 mM L-glutamine, 0.5 mM reduced glutathione, 0.5 mM sodium pyruvate, 0.3 mM sodium ascorbate, pH 7.4). Isolated retinas were mounted on filter paper (0.45 µm pore, mixed cellulose, Millipore) and flattened with gentle suction. After peeling away remaining RPE, flat-mounted retinas were sliced into 300-400 µm slices using a tissue slicer (Stoelting). Slices were rotated 90° and the filter paper edges buried in strips of wax on a coverslip for imaging at room temperature.

Fresh retinal slices were imaged at room temperature using a Leica SP8 confocal microscope with a 40X water objective; excitation/emission wavelengths were 488/525-575 nm for 2-NBDG, and 559/580-630 nm for tdTomato. Leica LAS-X (RRID:SCR_013673) software was used to acquire images at 2048 x 2048 pixel resolution with 12 bit depth, and Z-stacks imaged every 0.5 µm over a tissue depth of 10-30 µm.

Image analysis.

ImageJ software (RRID:SCR_002285) was used for quantification of 2-NBDG fluorescence in fresh retinal slices. 10 slices of each Z-stack were maximum intensity projected, and retinal layers were identified by morphology and expression of transgenic markers. For every slice, 3 small uniformly sized rectangular regions of interest (ROIs) were placed randomly in each retinal layer, and mean fluorescence intensity of each ROI was measured. Average 2-NBDG fluorescence in each layer was divided by the autofluorescence of corresponding retinal layers from animals gavaged with saline or water.

Metabolic flux analysis.

Isolated mouse retina or confluent human fetal RPE cells were changed into pre-warmed Krebs-Ringer Bicarbonate Buffer containing, depending on the experiment, [1,2] ^{13}C glucose, U-^{13}C glucose, U-^{13}C lactate or U-^{13}C glutamine (Sigma) as described elsewhere (Du et al., 2013a; 2015; 2016b). Both retinas and RPE cells were incubated for 5 min, 30 min, 60 min and 120 min. Metabolites from each time point were extracted and analyzed by gas chromatography mass spectrometry (GC-MS, Agilent 7890/5975C) as described in detail (Du et al., 2013a; 2013b).

Measurement of U-^{13}C glucose transport across hfRPE cells on transwell filters.

After maturation for 4-6 weeks in culture, hfRPE cells grown on transwell filters were changed into 500 µl of DMEM containing 1% FBS on each side. 5 mM U-^{13}C glucose (Cambridge Isotope Laboratories) was included in the medium in the basolateral side while various concentrations of sodium lactate was added to the apical side, while

maintaining a constant pH. Apical side medium was collected at 8 and 24 h to analyze the transported U-^{13}C glucose by liquid chromatography coupled with triple quadrupole mass spectrometry (Waters Xevo TQ Tandem mass spectrometer with a Waters ACQUITY system with UPLC) as reported in detail (Du et al., 2015).

Live-cell imaging (NAD(P)H autofluorescence. Cultured hfRPE cells were attached to cover slips that were previously coated with a thin layer of Matrigel (Corning, Corning NY) diluted 1:30 1-2 days prior to the imaging experiment. NAD(P)H was imaged and quantified similarly to a previous study (Jung et al., 2009). Cells were perfused with KRB (supplemented with 0.1% bovine serum albumin and 1% penicillin streptomycin fungizone (Invitrogen)) at a flow rate of ~0.1 ml/min at 37 °C on the stage of a Nikon Eclipse TE-200 inverted microscope. Fluorescence imaging of NAD(P)H was measured with emission detected at 460 nm by a CoolSnap HQ2 CCD camera (Photometrics, Tucson, AZ) through a 40x Super Fluor Nikon objective (DIC H/N2) during excitation at 360 nm via a Xenon lamp (Lambda LS-1620, Sutter Instrument Company, Novato, CA). NAD(P)H fluorescence integration time was 50 msec. The software package Elements (Nikon) was used to drive the data acquisition. At the completion of each protocol, the steady-state levels of relative fluorescence (RFU) during exposure of KCN and subsequently FCCP were measured and this data was used to normalize the relative fluorescence unit (RFU) data. The normalization of the NAD(P)H signal was as a percent of RFU_{FCCP} and RFU_{KCN}, defined as 0 and 100% respectively for each cell.

Serial Block Face Scanning EM

Mouse eyes were enucleated, the anterior half was dissected away, and the eyecup was cut in half. Tissue was fixed in 4% glutaraldehyde in 0.1 M sodium cacodylate buffer, pH 7.2, at room temperature (RT), then stored overnight at 4°C. Samples were washed 4 times in sodium cacodylate buffer, postfixed in osmium ferrocyanide (2% osmium tetroxide/3% potassium ferrocyanide in buffer) for 1 h on ice, washed, incubated in 1% thiocarbohydrazide for 20 min, and washed again. After incubation in 2% osmium tetroxide for 30 min at RT, samples were washed and en bloc stained with 1% aqueous uranyl acetate overnight at 4°C. Samples were finally washed and en bloc

stained with Walton's lead aspartate for 30 min at 60°C, dehydrated in a graded ethanol series, and embedded in Durcupan resin. Serial sections were cut at 60 nm thickness and imaged with 6 nm pixel size using a Zeiss Sigma VP scanning electron microscope fitted with a Gatan 3View2XP ultramicrotome apparatus. Imaged stacks were concatenated and aligned using TrakEM2 (RRID:SCR_008954). Unless stated otherwise, five washes with water were used for all wash steps.

Statistical analyses.

R (RRID:SCR_001905) with R Commander was used to perform one-way ANOVA for NBDG gavage experiments.

Reproducibility.

All data shown here have been reproduced at least three times by the authors.

Data availability.

All data supporting the findings of this study are available within the paper.

Acknowledgements.

The findings described in this chapter are published in eLife. Authors who contributed to this study are Mark A. Kanow (first author), Michelle M. Giarmarco, Connor SR Jankowski, Kristine Tsantilas, Abbi L. Engel, Jianhai Du, Jonathan D. Linton, Christopher C. Farnsworth, Stephanie R. Sloat, Austin Rountree, Ian R. Sweet, Ken J. Lindsay, Edward D. Parker, Susan E. Brockerhoff, Martin Sadilek, Jennifer R. Chao, James B. Hurley. This study was supported by funding from NIH EY06641 and NIH EY017863 to JBH, NIH EY026020 to SEB, NEI core grant EY001730 and P30 DK-17047 (Cell Function Analysis Core).

Chapter 3

Glycogen metabolism in the RPE and retina

Introduction

In fungi, bacteria, and animals glucose can be stored as a branched polysaccharide in the form of glycogen (Adeva-Andany et al., 2016; Berg et al., 2015; Shulman and Rothman 2001). Glycogen is mainly stored in muscle and liver tissue in humans, and is degraded into glucose monomers in order to maintain adequate blood glucose levels to support cellular viability and function. Everything from its catalytic breakdown (glycogenolysis) and storage of glycogen (glycogen synthesis) to the signaling cascades for its regulation have been extensively studied (Cori and Cori 1929; Cori et al., 1937; Sutherland and Wosilait 1955; 1956; Fischer and Krebs 1955; Krebs et al., 1958). During glycolysis, glucose-6-phosphate is converted to pyruvate which can be converted to lactate. In muscle tissue undergoing anaerobic glycolysis, excess lactate can be transported to the liver via the blood stream, and converted back to pyruvate (Cori cycle) for the production of glucose (gluconeogenesis). This glucose can be transported back to muscle tissue for use in glycolysis, or be stored as glycogen.

In the central nervous system, glycogen is mostly stored by astrocytes (Öz et al., 2015), and when the ability to store or break down glycogen is blocked it can lead to impaired learning and memory function (Duran et al., 2013; Suzuki et al., 2013; Gibbs et al., 2007; Hertz et al., 2003). In the retina, glycogen is primarily stored in Müller cell end feet (Shimizu et al., 1953), and the process of glycogen synthesis and glycogenolysis is regulated by an insulin-signaling pathway in the retina and primary cultures of MGCs (PérezLeón et al., 2013). It has been suggested that there exists a “Cori-like” cycle where MGCs can utilize lactate to synthesize glucose that can be stored as glycogen (Goldmann et al., 1986; 1987; Goldmann 1988; 1990). This glycogen can then be broken down into glucose monomers and exported out into the extracellular space for neighboring neurons and cells to use. Furthermore, MGCs lack any isoform of pyruvate kinase (PKM2), a necessary enzyme for the producing ATP in glycolysis (Lindsay et al.,

2014). Müller cells also express enolase, which is required for gluconeogenesis. The presence of enolase, and lack of PKM2 may enhance a gluconeogenic pathway.

RPE metabolism is primarily reliant on oxidative phosphorylation and amino acid oxidation (Chao et al., 2017; Du et al., 2016b; Kanow et al., 2017), and its ability to synthesize and breakdown glycogen is not well characterized. When grown in culture, adult human RPE can store glucose as glycogen under hyperglycemic conditions (deS Senanayake et al., 2006). This effect is also observed in human eyecups from diabetic donors, and is attributed to an increase in glycogen synthase activity (Hernandez et al., 2014). In the retina, it's possible for MGCs to store glucose as glycogen and break it down for feeding neighboring cells when glucose supply is low; however, it's not well studied whether the RPE can perform the same function for PRs of the retina.

We've identified an ecosystem model for RPE-retina metabolism where the RPE has a metabolic preference for lactate as a fuel substrate (Kanow et al., 2017). As a follow up to that study, we investigated: (1) whether the RPE could also utilize lactate as a substrate for gluconeogenesis and glycogen synthesis, and (2) confirmed the retina's ability to store glycogen. We developed a method for glycogen extraction in hfRPE, mEyecups, and mRetina, and an LCMS method for measuring the incorporation of carbons from U-^{13}C lactate or U-^{13}C glucose into glycogen. We confirmed that the RPE and mEyecups can store carbons from glucose as glycogen. The retina was able to store glucose as glycogen as well, albeit to a lesser extent than the RPE and mEyecups. When incubated in U-^{13}C lactate, hfRPE, mEyecups, nor mRetina was observed to incorporate carbons from lactate into glycogen. These findings suggest that the RPE and retina can store glucose as glycogen; however, gluconeogenesis may not be a primary pathway in either tissue.

Results

Mouse eyecups and retina are capable of storing glucose as glycogen

In vitro studies have shown that human RPE can store glucose as glycogen (deS Senanayake et al., 2006; Hernandez et al., 2014). We adapted a Methanol-HCl method for glycogen extraction from tissue (Lowry and Passonneau 1993) for use on mouse eyecups and retina, and confirmed previous findings that retina and RPE contain glycogen (Senanayake et al., 2006; Hernandez et al., 2014; PérezLeón et. al 2013, Pfeiffer et al 2005, and Rothermel et al 2008). We incubated freshly harvested mouse eyecups and retina in U^{13}C-glucose for 30min, 2hr, 6hr, and 18hr. Fig. 3.1 shows that both retina and eyecups incorporate glucose into glycogen over time. Mouse eyecups

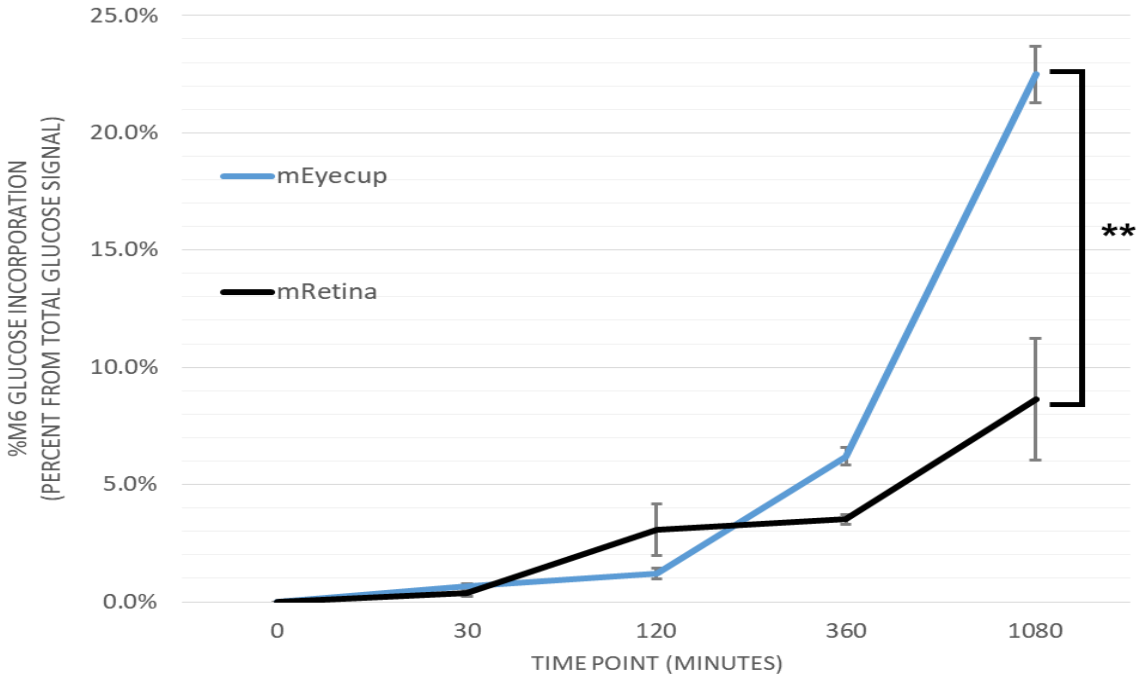

had an increased capacity for storing glycogen than mouse retina.

Fig. 3.1. Incorporation of U-^{13}C glucose into mEyecup and mRetina glycogen. mEyecups and mRetina were incubated in 10mM U-^{13}C glucose, and glycogen was extracted at 30min, 2hr, 6hr, and 18hr (n=3 for each time point). "M6 glucose" represents U-^{13}C glucose. %M6 glucose incorporation is illustrated as a percentage of M6 from the total amount of glucose stored as glycogen. Error bars report SE. **p<0.01

At the end of the time course, mEyecups had a 22.5 ± 1.2% (SE, n=3) incorporation of M6 glucose, while the retina displayed an 8.6 ± 2.6% (SE, n=3) incorporation.

Metabolically enhancing hfRPE's ability to store glucose into glycogen.

Given the RPE's metabolic preference for reductive carboxylation and proline as a nutrient source (Du et al., 2016b; Chao et al., 2017), we hypothesized that glutamine and/or proline can enhance the storage of glucose as glycogen. The presence of its preferred fuel source would not only allow for more glucose to be stored as glycogen, but perhaps fuel the process of glycogen synthesis as well.

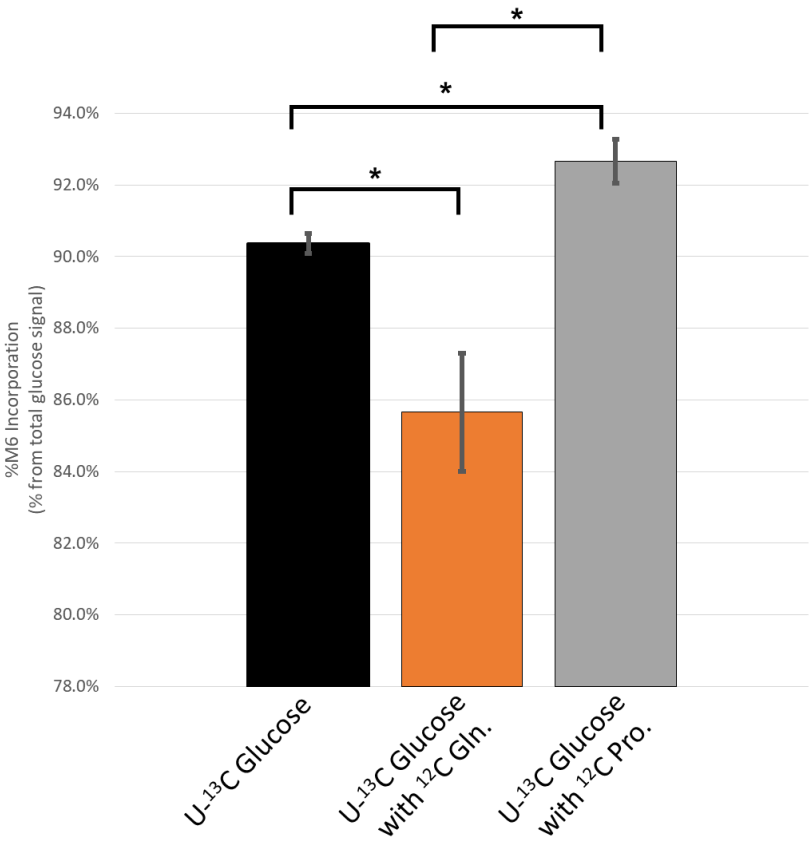

Fig. 3.2. Effects of glutamine (Gln.) and proline (Pro.) on glycogen synthesis in hfRPE. hfRPE were incubated in 10mM U-^{13}C glucose with 2mM ^{12}C Gln., or ^{12}C Pro. overnight (~18hr). %M6 glucose incorporation is illustrated as a percentage of M6 from the total amount of glucose stored as glycogen. Error bars report SE. *p<0.05

We found that 90.4 ± 0.28% (SE, n=3) of M6 glucose was incorporated into the total glucose from hfRPE glycogen. Incorporation of glucose into glycogen decreased to 85.7 ± 1.65% (SE, n=3) when ^{12}C glutamine was introduced in the presence of U-^{13}C glucose. ^{12}C proline was observed to increase the incorporation of M6 glucose at 92.7 ± 0.61% (SE, n=3).

Discussion

The enzymatic machinery necessary for glycogen synthesis and glycogenolysis in the retina is primarily distributed to Müller glial cells. MGCs possess glycogen phosphorylase and glycogen synthase, two vital components needed for glycogen metabolism (PérezLeón et. al 2013, Pfeiffer et al 2005, and Rothermel et al 2008). When imaged using light microscopy, the distribution of retinal glycogen is segregated to MGCs where the majority is stored in their end feet (Kuwabara et al 1961; Shimizu et al., 1953). Glycogen phosphorylase and synthase activity has also been characterized in human RPE (Hernandez et al., 2014). Furthermore, the RPE does store glucose as glycogen under hyperglycemic conditions (Senanayake et al., 2006; Hernandez et al., 2014). Taken together with the observations of nutrient preferences in the RPE and MGCs (Du et al., 2016b; Chao et al., 2017; Kanow et al., 2017; Lindsay et al., 2014; Riepe and Norenburg 1977), we proposed that the presence of certain fuels would enhance the storage of glucose as glycogen in the RPE and MGCs. In the experiments outlined in this study, the RPE is capable of more glycogen storage than the retina (Fig. 3.1). In the RPE, proline enhanced the storage of glucose as glycogen. A recent study showed that proline integrates into the TCA cycle in the RPE (Chao et al., 2017), which may be supplying the necessary energy substrates for glycogen synthesis and explain our findings in this study. Conversely, glutamine did not enhance glycogen synthesis in the RPE. One possible explanation for this could be the RPE's preference to use glutamine for fatty acid production (Du et al., 2016b). RPE derived fatty acids have been observed to supply the retina in the form of ketone bodies (Adijanto et al., 2014). A metabolic preference for fatty acid synthesis (via glutamine) would require the RPE to utilized ATP derived from glycolysis to fuel the process, consuming glucose that would otherwise be stored as glycogen.

Glycogen metabolism as part of the retinal ecosystem

Glucose disposal and glycogen metabolism begin with the transport of glucose into the cell. In the RPE, this is performed by GLUT1 (Kanow et al., 2017; Swarup et al., 2018; Badr et al., 2000; Gospe et al., 2010). Glycogen is the primary storage form of glucose, and its metabolism has been evaluated in this study. In the context of the retinal

ecosystem model, an obvious role for glycogen storage in the RPE would be as an emergency fuel source during hypoglycemic conditions, when circulating blood-glucose levels are low. The RPE could utilize stores of glycogen for feeding the retina to continue supplying the RPE with retinal lactate.

Potential fuels for enhanced glycogen metabolism

Although lactate is the preferred fuel source of the RPE (Kanow et al., 2017) and has been proposed to be a preferred fuel source for MGCs (Hurley et al., 2015), we did not see incorporation of carbons from lactate into retina or RPE derived glycogen (data not shown) when U-^{13}C lactate was used in place of U-^{13}C glucose in these studies. This suggests that gluconeogenesis may not be an enhanced pathway in the RPE or retina. Other fuels such as fatty acids (Joyal et al., 2016; Reyes-Reveles et al., 2017), ketone bodies (Adijanto et al., 2016), and other metabolites (Rueda et al., 2016; Swarup et al., 2018) have been highlighted to contribute to the metabolic specialization of the RPE and MGCs. Given that the retina exports significant amounts of lactate, future investigations should focus on whether lactate and these additional metabolites contribute to glycogen metabolism, and how this influences the metabolic ecosystem with respect to photoreceptor metabolism and retinal disease.

Materials and Methods

Animals

All research was authorized by the University of Washington Institutional Animal Care and Use Committee. Mice in the C57BL6J background were maintained in the University of Washington South Lake Union vivarium at 27.5 ºC on a 14h/10h light-dark cycle. C57BL/6J does not carry the rd8 mutation in the Crb1 gene (Mattapallil et al., 2012).

RPE cell culture

Human fetal eyes with a gestational age of 16-20 weeks were harvested and shipped overnight on ice in RPMI media containing antibiotics from Advanced Bioscience Resources Inc. (Alameda, CA). Dissections of fetal tissue were performed within 24

hours of procurement and followed a modified version of the dissection protocol in order to isolate the retinal pigment epithelium (RPE) (Sonoda et al., 2009). The fetal RPE sheets were incubated at 37°C with 5% CO_2 and cultured in RPE media. The RPE media consisted of Minimum Essential Medium alpha (Life Technologies) supplemented with 5% (vol/vol) fetal bovine serum (Atlanta Biologicals), N1-Supplement (Sigma-Aldrich), Nonessential Amino Acids (Gibco), and a Penicillin-Streptomycin solution (Gibco). Isolated fetal RPE reached confluency about 3-4 weeks after dissection and was then passaged using a 0.25% Trypsin-EDTA solution (Gibco) and passed through a 40 μm nylon cell strainer (BD Falcon) in order to collect a suspension of single cells. After counting, the RPE cells were plated onto 0.3 cm^2 cell culture inserts (Falcon) coated with Matrigel (Corning) at a seeding density of 100,000 cells per insert. Cells grown on these inserts were cultured in RPE media containing 1% (vol/vol) FBS. Transepithelial resistance was measured weekly after 2 weeks in culture using a Millicell ERS-2 Epithelial Volt-Ohm Meter (Millipore).

Glycogen extraction and flux analysis

Isolated mouse retina/eyecups or confluent human fetal RPE cells were changed into pre-warmed Krebs-Ringer Bicarbonate Buffer containing, depending on the experiment, ^{12}C glucose, ^{12}C glutamine, ^{12}C proline, U-^{13}C glucose, or U-^{13}C lactate (Sigma) as described elsewhere (Du et al., 2013a; 2015; 2016b; Chao et al., 2017). Mouse eyecups and retinas were incubated for 30 min, 2 hr, 6 hr, and 18 hr. RPE cells were incubated for 18 hr. Glycogen from each time point were extracted using ice cold 80% methanol. Glycogen pellets were washed three times with ice cold 80% methanol before glycogen hydrolysis was performed. For hydrolysis, glycogen was heated for 1 hr at 80˚C in 1N HCl. The hydrolysis reaction was neutralized using an equivalent amount of 1N NH_5CO_3. Total reaction was diluted 50-fold in methanol for free glucose extraction. Glucose extracts were centrifuged and dried down as described in detail (Du et al., 2013a; 2013b). U-^{13}C glucose incorporation was measured by liquid chromatography coupled with triple quadrupole mass spectrometry (Waters Xevo TQ Tandem mass spectrometer with a Waters ACQUITY system with UPLC) as reported in detail (Du et al., 2015).

Statistical analyses.

R (RRID:SCR_001905) with R Commander was used to perform Wilcoxon signed rank test for hfRPE glycogen experiments.

Reproducibility.

All data shown here have been reproduced at least two times.

Data availability.

All data supporting the findings of this study are available within the paper.

Acknowledgements.

The findings described in this chapter are unpublished. Individuals who contributed to this study are Mark A. Kanow, Abbi L. Engel, Martin Sadilek, Jennifer R. Chao, and James B. Hurley. This study was supported by funding from NIH EY06641 and NIH EY017863 to JBH.

Chapter 4

Developing an LC-MS method for detecting metabolites in glycolysis

Introduction

Large and small molecule organic phosphates are relevant to metabolic flux analyses, and can be difficult compounds to analyze. They exist in many metabolic processes such as glycolysis. Glycolysis is a multi-enzymatic sequence of ten reactions that convert glucose to pyruvate ultimately producing the high-energy molecule ATP. Vertebrate retinas produce a lot of these compounds as they are highly glycolytic (Krebs 1927; Warburg et al., 1924; Wang et al., 1997). Analysis of the glycolytic intermediate metabolites in the retina has been mostly by gas chromatography mass spectrometry (Du et al., 2013a; 2013b; 2015; 2016a; Kanow et al., 2017; Lindsay et al., 2014). This technique requires the derivatization of analytes so they can be volatized and separated via gas chromatography. Caveats to this method are: samples are not storable long term after derivatization due to water hydrolysis (Gunnar et al., 2005; Adiels et al., 2010), and turnaround time for sample prep and runtimes are time intensive. It has been shown that large and thermo-unstable organic molecules like sugars, phosphates and nucleotides can be detected from the retina using liquid chromatography mass spectrometry (Du et al., 2015). Samples analyzed using LC-MS did not require derivatization in that study, and metabolite detection sensitivity and stability was unchanged or improved compared to GC-MS techniques. The purpose of this study was to develop an LC-MS method for detecting glycolytic intermediates that would be as robust as current GC-MS methods, and could be applied to metabolic flux studies in the retina/RPE for more rapid turnaround and efficiency for on-going studies.

Protocol and Spectra

Sample preparation for LC-MS analysis

Table 4.1 summarizes the detection parameters for the glycolytic intermediates: gluose-6-phosphate (G6P), fructose-1,6-bisphosphate (F16BP), glyceraldehyde-3-phosphate (GAP), dihydroxyacetone phosphate (DHAP), 3-phosphoglycerate (3PG), and phosphoenol pyruvate (PEP) were prepared in 200µL of mobile phase for multiple

reaction monitoring (MRM) method development in LC-MS. A Waters Xevo TQ Tandem mass spectrometer with a Waters ACQUITY system with UPLC was used for analyzing metabolites for LC-MS. For chromatographic separation, an ACQUITY UPLC BEH Amide analytic column (2.1 X 50mm, 1.7µm, Waters) was used.

Table 4.1. Glycolytic intermediate metabolites for LCMS analysis.

Metabolite	Mode	Parent (*m/z*)	Daughter (*m/z*)	Dwell (s)	Cone (V)	Collison (eV)
G6P	Negative	258.97	96.91	0.100	44.00	16.00
F16BP	Negative	339.03	96.90	0.010	26.00	14.00
GAP	Negative	168.95	96.90	0.100	15.00	13.00
DHAP	Negative	168.90	96.95	0.100	17.00	11.00
3PG	Negative	184.95	96.90	0.100	18.00	14.00
PEP	Negative	166.90	78.90	0.100	15.00	13.00

The mobile phase is (A) water with 10mM ammonium bicarbonate (pH 9.1), 0.8% ammonium hydroxide and (B) acetonitrile/water (95/5%) with 10mM ammonium bicarbonate (pH 9.1), 0.8% ammonium hydroxide. All solvents are LC-MS optima grade from Fisher Scientific. Gradient elution is (1) 95 – 65% B in 2.3 min, (2) 65 – 30% B at 2.8 min, and (3) 30 – 95% B at 3.3 min. The column is re-equilibrated with 95% B at the end of every run. Flow rate for all gradients is 0.4 ml/min, and the total run time is 8 min. Sample injection volume is 5 µl. Mass spectrometer settings are shown in Table 4.1 where each transition shows a parent ion and fragmented daughter ion. Knowledge of the transition and labeling patterns can be checked in public databases such as MoNA (http://mona.fiehnlab.ucdavis.edu/), Human Metabolome Database (http://www.hmdb.ca/), and METLIN (http://metlin.scripps.edu/index.php). The chromatographs (Fig. 4.1.) were analyzed using MassLynx V4.1 (Waters). Alternative mobile phases using an ammonium acetate salt (as describe in Du et al., 2015) were tested as well; however, peak shape and retention was not adequate for quantitation.

For applications in retina metabolism studies, sample collection and preparation require quick reaction quenching, and an effective extraction method for metabolites that have a

very rapid turnover in the cell. There are many investigations on quenching reactions and extracting cellular metabolites. We have observed cold saline to be optimal for reaction quenching, and extracting polar metabolites with cold methanol (Strumilo 1995; Lu et al., 2017; Zhu et al., 2018). *Ex vitro* retina samples are washed in cold 0.9% NaCl to quench metabolism, and tissue is immediately frozen in liquid nitrogen. Frozen tissue samples are then homogenized in an extraction buffer (80% methanol) that's been store on ice. The homogenate is then centrifuged at 14,000 rpm for 30 min at 4˚C, and the supernatant containing metabolites is extracted and dried down. Supernatant samples are dried for mass spectrometry to remove methanol and water so that metabolites can be reconstituted in 200µL of mobile phase for LC-MS.

Discussion

Applications of this metabolite detection strategy can be directly applied for investigating retina/RPE metabolism in the eye. Fig. 4.1 highlights the total ion chromatographs for the metabolites listed in Table 4.1. We were able to achieve chromatographic separation between the hexose phosphate sugars, G6P and F16P (Fig. 4.1). There is some peak overlap between the two metabolites; however, the *m/z* transitions allow for differentiation between the two molecules.

Retention times between the smaller molecule phosphates were 1.34 min (GAP), 1.29 min (DHAP), 1.33 min (3PG), and 1.32 min (PEP) and proved to be more difficult to separate via chromatography. Of the small molecule phosphates, 3PG and PEP have masses that differ significantly which makes them relatively easy to identify when quantifying their target ions. In contrast, GAP and DHAP possess identical *m/z* ratios which do not allow for clear differentiation between the two. If this method were to be used for metabolic flux studies, then a combined metabolite pool of GAP-DHAP would have to be used for analysis. The above methods have also been previously applied towards metabolites such as: pyruvate, lactate, and glucose (data not shown).

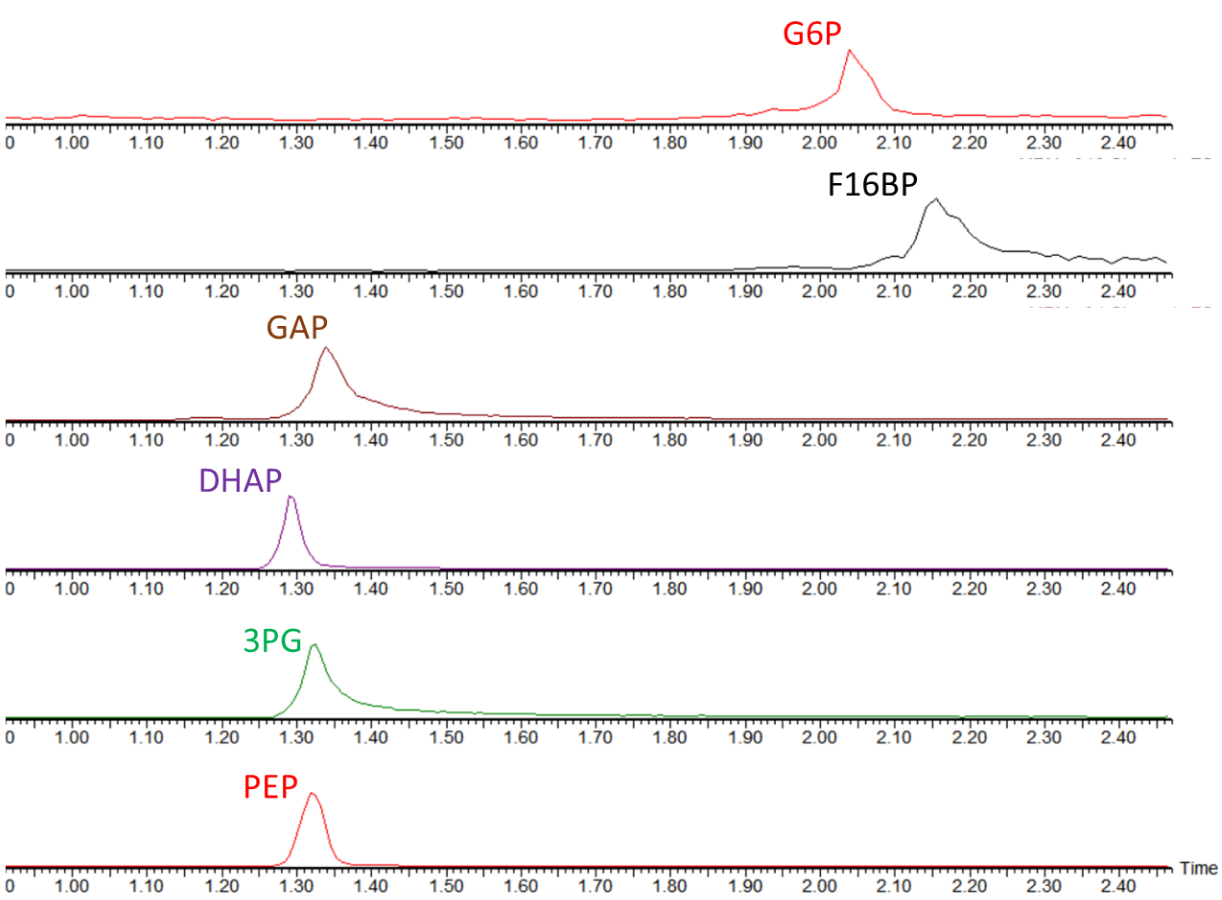

Fig. 4.1. Glycolytic intermediate total ion chromatographs. G6P, glucose-6-phosphate; F16BP, fructose-1,6-bisphosphate; GAP, glyceraldehyde-3-phosphate; DHAP, dihydroxyacetone phosphate; 3PG, 3-phosphoglycerate; PEP, phosphoenol pyruvate. Retention time (x-axis) represented in minutes.

Improving chromatography

The present method proved to be robust for glycolytic flux studies. Metabolites from Table 4.1 were detected; however, separation of the smaller molecule phosphates could be improved. The chromatography in this study was performed using a BEH Amide column, which utilizes an ethylene bridged hybrid particle as a solid phase. The BEH Amide particles are able to retain polar analytes and metabolites. Improved separation would be obtained with a longer column. Additionally, an option for better detection and separation that was not investigated in this study would be an alternative solid phase for analyte and metabolite retention. A zwitterionic stationary phase covalently attached to porous silica is suitable for hydrophilic interaction liquid chromatography (ZIC-HILIC). Such methods have been used successfully for separation and detecting nucleotides,

amino acids, sugar phosphates, and carboxylic acids (Contrepois et al., 2015; Marrubini et al., 2013; Greco et al., 2013).

Reproducibility.

All data shown here have been reproduced at least three times.

Data availability.

All data supporting the findings of this study are available within the paper.

Acknowledgements.

The findings described in this chapter are unpublished. Individuals who contributed to this study are Mark A. Kanow, Martin Sadilek, Kristine Tsantilas, Celia Bisbach, and James B. Hurley. This study was supported by funding from NIH EY06641 and NIH EY017863 to JBH.

Chapter 5

Conclusions and Future Directions

Metabolic specializations between the RPE and photoreceptors

Glucose is the immediate energy substrate of the retina, and must first traverse the RPE through glucose transporters before it can reach the retina. The RPE is known to use MCTs for nutrient and waste removal in the eye (Yoon et al., 1997; Bergersen et al., 1999). Here we show that the primary glucose transporter for the RPE and retina is GLUT1 (Fig. 2.1), and that glucose primarily enters the retina via photoreceptors (Fig. 2.2). The retina converts significant amounts of glucose to lactate (Fig.2.4), and the RPE uses MCTs to import lactate which is then oxidized to pyruvate and used to fuel oxidative phosphorylation (Fig. 2.5, Fig. 2.6). The oxidation of lactate requires reduction of NAD^+, a required cofactor for glycolysis, to NADH (Fig. 2.7). With reduced pools of NAD^+, glycolysis becomes attenuated in the RPE (Fig. 2.8). This allows for more glucose to diffuse towards the retina (Fig. 2.9). When this working model (Fig. 2.10) for the “metabolic ecosystem” is perturbed, it may contribute to some forms of retinal disease and degeneration.

The RPE in this working model for retina metabolism serves as a unique transporter of glucose. A key highlight of this function requires glucose to flow through the RPE towards the retina without being consumed. This unique behavior does not only apply to eye metabolism, but also to different tissues and organs. Examples of other cell types that serve in a similar capacity (glucose transport without consumption) are the epithelial cells in mammary glands, small intestine, and in the renal outer cortex and medulla of the kidneys (Wright 2013; Wright et al., 2011; Zhao and Keating 2007).

Glycogen as part of the metabolic ecosystem

An RPE preference for lactate as a fuel source, and MGC distribution of glycogen (Kuwabara et al., 1961; Shimizu et al., 1953) led us to follow up on the role of gluconeogenesis and glycogen metabolism in the RPE and retina and their potential contribution to our working ecosystem model. We did not observe detectable

incorporation of carbons from U-^{13}C lactate into RPE and retinal glycogen (data not shown), which indicated that gluconeogenesis may not be an enhanced pathway in either tissues. Even though gluconeogenesis may not be a pathway in RPE and retina, glycogen metabolism appeared to be present in both with the RPE being capable of storing significantly more glycogen (Fig. 3.1 and Fig. 3.2). The simplest explanation for glycogen metabolism in the RPE is that it serves as an emergency storage system for retinal glucose when blood glucose levels are low. Glycogen stores would be broken down to feed the retina, which would continue supplying lactate to the RPE.

How do alternative metabolites influence glycogen, RPE and retina metabolism?
Proline and glutamine were investigated in this study with proline serving to enhance glycogen storage in the RPE (Fig. 3.2). Fuels such as fatty acids, ketone bodies, and additional amino acids have been revealed to be alternative sources of nourishment for the RPE and retina (Joyal et al., 2016; Reyes-Reveles et al., 2017; Adijanto et al., 2016; Swarup et al., 2018), and may serve as alternative pathways that provide the necessary energy for glycogen synthesis. Many questions remain unanswered with regard to how these different fuels influence glycogen and eye metabolism, and their contribution to retinal diseases. Future studies that exploit their availability to the eye may help shed light on glycogen's role in the metabolic ecosystem.

References

Ablonczy Z, Dahrouj M, Tang PH, Liu Y, Sambamurti K, Marmorstein AD, et al. (2011). Human retinal pigment epithelium cells as functional models for the RPE in vivo. Invest Ophthalmol Vis Sci. 52(12):8614-20.

Adeva-Andany, M.M., Gonzalez-Lucan, M., Donapetry_Garcia, C., Fernandez, C., Amerneiros-Rodriguez, E. (2016). Glycogen metabolism in humans. BBA Clinical. 5: 85 – 100.

Adiels, M., Larsson, T., Sutton, P. et al. (2010). Optimization of N-methyl-N-[tert-butyldimethylsilyl]-trifluoroacetamide as a derivatization agent for determing isotopic enrichment of glycerol in very-low density lipoproteins. Rapid Comm Mass Spec. 24: 586 – 592.

Adijanto, J., Banzon, R., Jalickee, S., Wang, N.S., and Miller, S.S. (1997). CO_2-induced ion and fluid transport in human retinal pigment epithelium. The Journal of General Physiology 133(6): 603-622.

Adijanto J, Du J, Moffat C, Seifert EL, Hurley JB, Philp NJ. (2014). The retinal pigment epithelium utilizes fatty acids for ketogenesis. J Biol Chem. 289(30):20570-82.

Adijanto J, Philp NJ. (2014). Cultured primary human fetal retinal pigment epithelium (hfRPE) as a model for evaluating RPE metabolism. Exp Eye Res. 126:77-84.

Aït-Ali, N., Fridlich, R., Millet-Puel, G., Clérin, E., Delalande, F., Jaillard, C., Blond, F., Perrocheau, L., Reichman, S., Byrne, L.C., Olivier-Bandini, A., Bellalou, J., Moyse, E., Bouillaud, F., Nicol, X., Dalkara, D., Van Dorsselaer, A., Sahel, J.A., and Léveillard, T. (2015). Rod-Derived Cone Viability Factor Promotes Cone Survival by Stimulating Aerobic Glycolysis. Cell 161(4):817-32.

Akimoto M, Cheng H, Zhu D, Brzezinski JA, Khanna R, Filippova E, et al. (2006). Targeting of GFP to newborn rods by Nrl promoter and temporal expression profiling of flow-sorted photoreceptors. Proc Natl Acad Sci U S A. 103(10):3890-5.

Arshavsky, V.Y., Lamb, T.D., and Pugh, E.N. (2002). G Proteins and phototransduction. Annu. Rev. Physiol. 64:153 – 87

Badr GA, Tang J, Ismail-Beigi F, Kern TS. (2000). Diabetes downregulates GLUT1 expression in the retina and its microvessels but not in the cerebral cortex or its microvessels. Diabetes. 49(6):1016-21.

Berg, J.M., Tymockzko, J.L., Gatto, G.J., Stryer, L. (2015). Biochemistry, 8th Ed. W.H. Freeman & Company.

Bergersen, L., Johannsson, E., Veruki, M.L., Nagelhus, A., Halestrap, A., Sejersted, O.M., and Ottersen, O.P. (1999). Cellular and Subcellular Expression of

Monocarboxylate Transporters in the Pigment Epithelium and Retina of the Rat. Neuroscience 90(1): 319-331.

Blenkinsop TA, Saini JS, Maminishkis A, Bharti K, Wan Q, Banzon T, et al. (2015). Human Adult Retinal Pigment Epithelial Stem Cell-Derived RPE Monolayers Exhibit Key Physiological Characteristics of Native Tissue. Invest Ophthalmol Vis Sci. 56(12):7085-99.

Bonilha, V.L. (2014). Retinal pigment epithelium (RPE) cytoskeleton in vivo and in vitro. Experimental eye research. 126C: 38 – 45.

Bringmann, A., Pannicke, B., Biedermann, B., Francke, M., Isandiev, I., Grosche, J., Wiedemann, P., Albrecht, J., and Reichenbach, A. (2009). Role of retinal glial cells in neurotransmitter uptake and metabolism. Neurochemistry International 54(3-4): 143-160.

Casson RJ, Wood JP, Han G, Kittipassorn T, Peet DJ, Chidlow G. (2016). M-Type Pyruvate Kinase Isoforms and Lactate Dehydrogenase A in the Mammalian Retina: Metabolic Implications. Invest Ophthalmol Vis Sci. 57(1):66-80.

Chao JR, Knight K, Engel AL, Jankowski C, Wang Y, Manson MA, et al. (2017). Human retinal pigment epithelial cells prefer proline as a nutrient and transport metabolic intermediates to the retinal side. J Biol Chem. 292(31):12895-905.

Chinchore Y, Begaj T, Wu D, Drokhlyansky E, Cepko CL. (2017). Glycolytic reliance promotes anabolism in photoreceptors. Elife. 6

Collymore C, Rasmussen S, Tolwani RJ. (2013). Gavaging adult zebrafish. J Vis Exp. (78)

Contrepois, K., Jiang, L., and Snyder, M. (2015). Optimized Analytical Procedures for the Untargeted Metabolomic Profiling of Human Urine and Plasma by Combining Hydrophilic Interaction (HILIC) and Reverse-Phase Liquid Chromatography (RPLC)-Mass Spectrometry. Mol Cell Proteomics. 14(6):1684 – 95.

Coorey, N.J., Shen, W., Chung, S.H., Zhu, L., Gillies, M.C. (2012). The role of glia in retinal vascular disease. Clinical and Experimental Optometry 95:266-281.

Cori, C.F., and Cori, G.T. (1929). Glycogen formation in the liver from d- and l-lactic acid. Journal of Biological Chemistry. 81:389 – 403.

Cori, C.F., Colowick, S.P., and Cori, G.T. (1937). The isolation and synthesis of glucose-1-phosphoric acid. Journal of Biological Chemistry. 121:465 – 477

Cori, C.F., Schmidf, G. and Cori, G.T. (1939). The synthesis of a polysaccharide from gluose-1-phosphate in muscle extract. Science. 89:464 – 465.

De Melo Reis, R.A., Marques Ventura, A. L., Schitine, C.S., de Mello, M.C.F., de Mello, F.G. (2008). Müller Glia as an Active Compartment Modulating Nervous Activity in the

Vertebrate Retina: Neurotransmitters and Trophic Factors. Neurochem. Res. 33:1466 – 1474.

deS Senanayake, P., Calabro, A., Hu, J.G., Bonilha, V.L., Darr, A., Bok, D., Hollyfield, J.G. (2006). Glucose utilization by the retinal pigment epithelium: Evidence for rapid uptake and storage in glycogen, followed by glycogen utilization. Experimental Eye Research. 83: 235 – 246.

Du, Jianhai., Cleghorn, W., Contreras, L., Linton, J.D., Chan, G.C-K., Chertov, A. O., Saheki, T., Govindaraju, V., Sadilek, M., Satrústegui, J., and Hurley, J.B. (2013a).. Cytosolic reducing power preserves glutamate in retina. Proceedings of the National Academy of Sciences of the United States of America 110(46): 18501-18506.

Du J, Cleghorn WM, Contreras L, Lindsay K, Rountree AM, Chertov AO, et al. (2013b). Inhibition of mitochondrial pyruvate transport by zaprinast causes massive accumulation of aspartate at the expense of glutamate in the retina. J Biol Chem. 288(50):36129-40.

Du J, Linton JD, Hurley JB. (2015). Probing Metabolism in the Intact Retina Using Stable Isotope Tracers. Methods Enzymol. 561:149-70.

Du J, Rountree A, Cleghorn WM, Contreras L, Lindsay KJ, Sadilek M, et al. (2016a). Phototransduction Influences Metabolic Flux and Nucleotide Metabolism in Mouse Retina. J Biol Chem. 291(9):4698-710.

Du J, Yanagida A, Knight K, Engel AL, Vo AH, Jankowski C, et al. (2016b). Reductive carboxylation is a major metabolic pathway in the retinal pigment epithelium. Proc Natl Acad Sci U S A. 113(51):14710-5.

Duran, J., Saez, I., Gruart, A., Guinovart, J.J., and Delgado-Garcia, J.M. (2013). Impairment in long-term memory formation and learning-dependent synaptic plasticity in mice lacking glycogen synthase in the brain. Journ Cereb Blood Flow Metab. 33: 550 – 556.

Fischer, E.H., and Krebs, E.G. (1955). Conversion of phosphorylase b to phosphorylase a in muscle extracts. Journal of Biological Chemistry. 216: 121 – 132.

Giarmarco MM, Cleghorn WM, Sloat SR, Hurley JB, Brockerhoff SE. (2017). Mitochondria maintain distinct Ca2+ pools in cone photoreceptors. J Neurosci. 37(8):2061 – 2072.

Gibbs, M.E., Lloyd, H.G., Santa, T., and Hertz, L. (2007). Glycogen is a preferred glutamate precursor during learning in 1-day old chick: biochemical and behavioral evidence. Journal of Neuroscience Research. 85: 3326 – 3333.

Goldman, S.S., and Witkovsky, P. (1986). Glycogen Metabolism in an Amphibian Retina. Experimental Eye Research 43: 267-272.

Goldman, S.S., and Witkovsky, P. (1987). Evidence for Gluconeogenesis in the Amphibian Retina. Experimental Eye Research 44: 65-71.

Goldman, S.S. (1988). Gluconeogenesis in the amphibian retina. Lactate is preferred to glutamate as the gluconeogenic precursor. The Biochemical Journal 254(2): 359-365.

Goldman, S.S. (1990). Evidence that the Gluconeogenic Pathway is Confined to an Enriched Müller Cell Fraction Derived from the Amphibian Retina. Experimental Eye Research 50: 213-218.

Gospe SM, 3rd, Baker SA, Arshavsky VY. (2010). Facilitative glucose transporter Glut1 is actively excluded from rod outer segments. J Cell Sci. 123(Pt 21):3639-44.

Greco, G., Grosse, S., Letzel, T. (2013). Serial coupling of reversed-phase and zwitterionic hydrophilic interaction LC/MS for the analysis of polar and nonpolar phenols in wine. J Sep Sci. 36:1379-1388.

Gunnar, T., Ariniemi, K., Lillsunde, P. (2005). Determination of 14 benzodiazepines and hydroxy metabolites, zaleplon, and zolpidem as tert-butyldimethylsilyl derivatives compared with other common silyating reagents in whole blood by gas chromatography-mass spectrometry. Jour Chromatography. 818: 175 – 189.

Heitzmann, H. (1972). Rhodopsin is the predominant protein of rod outer segment membranes. Nat New Biol. 235(56):114.

Hernandez, C., Garcia-Ramirez, M., Garcia-Rocha, M., Saez-Lopez, C., Valverde, A.M., Guinovart, J.J., Simo, F. (2014). Glycogen storage in the human retinal pigment epithelium a comparative study of diabetic and non-diabetic donors. Acta Diabetol. 51: 543 – 552.

Hertz, L., O'Dowd, B.S., Ng, K.T., and Gibbs, M.E. (2003). Reciprocal changes in forebrain contents of glycogen and of glutamate/glutamine during early memory consolidation in the day-old chick. Brain Research. 994: 226 – 233.

Hung YP, Albeck JG, Tantama M, Yellen G. (2011). Imaging cytosolic NADH-NAD(+) redox state with a genetically encoded fluorescent biosensor. Cell Metab. 14(4):545-54.

Hurley JB, Lindsay KJ, Du J. (2015). Glucose, lactate, and shuttling of metabolites in vertebrate retinas. J Neurosci Res. 93(7):1079-92.

Johnson LV, Forest DL, Banna CD, Radeke CM, Maloney MA, Hu J, et al. (2011). Cell culture model that mimics drusen formation and triggers complement activation associated with age-related macular degeneration. Proc Natl Acad Sci U S A. 108(45):18277-82.

Joyal JS, Sun Y, Gantner ML, Shao Z, Evans LP, Saba N, et al. (2016). Retinal lipid and glucose metabolism dictates angiogenesis through the lipid sensor Ffar1. Nat Med. 22(4):439-45.

Jung SR, Reed BJ, Sweet IR. (2009). A highly energetic process couples calcium influx through L-type calcium channels to insulin secretion in pancreatic beta-cells. Am J Physiol Endocrinol Metab. 297(3):E717-27.

Kevany, B.M., and Palczewski, K. (2010). Phagocytosis of Retinal Rod and Cone Photoreceptors. Physiology 25(60): 8-15.

Koch SF, Duong JK, Hsu CW, Tsai YT, Lin CS, Wahl-Schott CA, et al. (2017). Genetic rescue models refute nonautonomous rod cell death in retinitis pigmentosa. Proc Natl Acad Sci U S A. 114(20):5259-64.

Kolb, H. (1991). The neural organization of the human retina. In: Heckenlively JR, Arden GB, editors. Principles and practices of clinical electrophysiology of vision. St. Louis: Mosby Year Book Inc.; p. 25-52.

Kolb, H. (2005). Glial Cells of the Retina. In: Kolb, H., Nelson, R., Fernandez, E., Jones, B., WEBVISION The organization of the retina and visual system. http://webvision.med.utah.edu.

Kolko M, Vosborg F, Henriksen UL, Hasan-Olive MM, Diget EH, Vohra R, et al. (2016). Lactate Transport and Receptor Actions in Retina: Potential Roles in Retinal Function and Disease. Neurochem Res. 41(6):1229-36.

Krebs, E.G., Kent, A.B., and Fischer, E.H. (1958). The muscle phosphorylase b kinase reaction. Journal of Biological Chemistry. 231: 73 – 83.

Krebs HA. (1927). On the metabolism of the retina. Biochemische Zeitschrift. 189:57-9.

Kurihara T, Westenskow PD, Gantner ML, Usui Y, Schultz A, Bravo S, et al. (2016). Hypoxia-induced metabolic stress in retinal pigment epithelial cells is sufficient to induce photoreceptor degeneration. Elife. 5.

Kuwabara, T., and Cogan, D. G. (1961). Retinal Glycogen. Transactions of the American Ophthalmological Society 59:106-110.

Lamb, T.D., and Pugh, E.N. (2004). Dark adaptation and the retinoid cycle of vision. Progress in Retinal and Eye Research 23: 307-380.

Lehmann GL, Benedicto I, Philp NJ, Rodriguez-Boulan E. (2014). Plasma membrane protein polarity and trafficking in RPE cells: past, present and future. Exp Eye Res. 126:5-15.

Lewis A, Williams P, Lawrence O, Wong RO, Brockerhoff SE. (2010). Wild-type cone photoreceptors persist despite neighboring mutant cone degeneration. J Neurosci. 30(1):382-9.

Li, Q., and Puro, D.G. (2002). Diabetes-Induced Dysfunction of the Glutamate Transporter in Retinal Müller Cells. Investigative Ophthalmology & Visual Science 43(9): 3109-16.

Lindsay, K.J., Du, J., Sloat, S.R., Contreras, L., Linton, J.D., Turner, S.J., Sadilek, M., Satrustegui, J., Hurley, J.B. (2014). Pyruvate kinase and aspartate-glutamate carrier distributions reveal key metabolic links between neurons and glia in retina. Proceedings

of the National Academy of Sciences of the United States of America 111(43): 15579-15584.

Linton JD, Holzhausen LC, Babai N, Song H, Miyagishima KJ, Stearns GW, et al. (2010). Flow of energy in the outer retina in darkness and in light. Proc Natl Acad Sci U S A. 107(19):8599-604.

Lowry, O.H., and Passanneau, J.V. (1993). Enzymatic Analysis: A Practical Guide. The Human Press Inc. p. 76.

Lowry, O. H., Roberts, N. R., Schulz, D. W., Clow, J. E., and Clark, J. R. (1961). Quantitative Histochemistry of Retina. The Journal of Biological Chemistry 236(10): 2813-2821.

Lu, W., Su, X., Klein, M.S., Lewis, I.A., Fiehn, O., Rabinowitz, J.D. (2017). Metabolite Measurement: Pitfalls to Avoid and Practices to Follow. Annu Rev Biochem. 86: 277 – 304.

Marrubini, G., Pedrali, A., Hemstrom, P., Jonsson, T., Appelblad, P., Massolini, G. (2013). Column comparison and method development for the analysis of short-chain carboxylic acids by zwitterionic hydrophilic interaction liquid chromatography with UV detection. J Sep Sci. 36:3493-3502.

Matschinsky FM, Passonneau JV, Lowry OH. (1968). Quantitative histochemical analysis of glycolytic intermediates and cofactors with an oil well technique. J Histochem Cytochem. 16(1):29-39.

Mattapallil MJ, Wawrousek EF, Chan CC, Zhao H, Roychoudhury J, Ferguson TA, et al. (2012). The Rd8 mutation of the Crb1 gene is present in vendor lines of C57BL/6N mice and embryonic stem cells, and confounds ocular induced mutant phenotypes. Invest Ophthalmol Vis Sci. 53(6):2921-7.

Medrano CJ, Fox DA. (1995). Oxygen consumption in the rat outer and inner retina: light- and pharmacologically-induced inhibition. Exp Eye Res. 61(3):273-84.

Metallo CM, Walther JL, Stephanopoulos G. (2009). Evaluation of 13C isotopic tracers for metabolic flux analysis in mammalian cells. J Biotechnol. 144(3):167-74.

Öz, G., DiNuzzo, M., Kumar, A., Moheet, A., and Seaquist, E.R. (2015). Revisiting glycogen content in the human brain. Neurochem Res. 40: 2473 – 2481.

Papermaster, D.S. and Dreyer, W.J. (1974). Rhodopsin content in the outer segment membranes of bovine and frog retinal rods. Biochemistry. 13(11): 2438 – 44.

PérezLeón, J. A., Osorio-Paz, I., Francois, L., Salceda, R. (2013). Immunohistochemical Localization of Glycogen Synthase and GSK3β: Control of Glycogen Content in Retina. Neurochemical Research 38(5): 1063-1069.

Pfeiffer-Guglielmi, B., Francke, M., Reichenbach, A., Fleckenstein, Burkhard., Jung, G., and Hamprecht, B. (2005). Glycogen Phosphorlyase Isozyme Pattern in Mammalian Retinal Müller (Glial) Cells and in Astrocytes of Retina and Optic Nerve. Glia 49: 84-95.

Punzo C, Xiong W, Cepko CL. (2012). Loss of daylight vision in retinal degeneration: are oxidative stress and metabolic dysregulation to blame? J Biol Chem. 287(3):1642-8.

Punzo C, Kornacker K, Cepko CL. (2009). Stimulation of the insulin/mTOR pathway delays cone death in a mouse model of retinitis pigmentosa. Nat Neurosci. 12(1):44-52.

Rajala, A., Cupta, V.K., Anderson, R.E., Rajala, R.V.S. (2013). Light activation of the insulin receptor regulates mitochondrial hexokinase. A possible mechanism of retinal neuroprotection. Mitochondrion 13(6): 566-576.

Rajala RV, Rajala A, Kooker C, Wang Y, Anderson RE. (2016). The Warburg Effect Mediator Pyruvate Kinase M2 Expression and Regulation in the Retina. Sci Rep. 6:37727.

Raymond PA, Colvin SM, Jabeen Z, Nagashima M, Barthel LK, Hadidjojo J, et al. (2014). Patterning the cone mosaic array in zebrafish retina requires specification of ultraviolet-sensitive cones. PLoS One. 9(1):e85325.

Reichenbach A, and Bringmann A. (2013). New functions of Muller cells. Glia 61(5):651-678.

Reyes-Reveles J, Dhingra A, Alexander D, Bragin A, Philp NJ, Boesze-Battaglia K. (2017). Phagocytosis Dependent Ketogenesis in Retinal Pigment Epithelium. J Biol Chem.

Riepe RE, Norenburg MD. (1977). Muller cell localization of glutamine synthetase in rat retina. Nature. 268(5621):654-5.

Rothermel, A., Weigel, W., Pfeiffer-Guglielmi, B., Hamprecht, B., Robitzki, A. (2008). Immunocytochemical Analysis of Glycogen Phosphorylase Isozymes in the Developing and Adult Retina of the Domestic Chicken (*Gallus domesticus*). Neurochemical Research 33: 336-347.

Rueda EM, Johnson JE, Jr., Giddabasappa A, Swaroop A, Brooks MJ, Sigel I, et al. (2016). The cellular and compartmental profile of mouse retinal glycolysis, tricarboxylic acid cycle, oxidative phosphorylation, and ~P transferring kinases. Mol Vis. 22:847-85.

Santos LRB, Muller C, de Souza AH, Takahashi HK, Spegel P, Sweet IR, et al. (2017). NNT reverse mode of operation mediates glucose control of mitochondrial NADPH and glutathione redox state in mouse pancreatic beta-cells. Mol Metab. 6(6):535-47.

Senanayake P, Calabro A, Hu JG, Bonilha VL, Darr A, Bok D, et al. (2006). Glucose utilization by the retinal pigment epithelium: evidence for rapid uptake and storage in glycogen, followed by glycogen utilization. Exp Eye Res. 83(2):235-46.

Shimizu, N., and Maeda, S. (1953). Histochemical Studies on Glycogen of The Retina. Anatomical Record 116(4): 427-437.

Shin J, Chen J, Solnica-Krezel L. (2014). Efficient homologous recombination-mediated genome engineering in zebrafish using TALE nucleases. Development. 141(19):3807-18.

Shulman, R.G. and Rothman, D.L. (2001). 13C NMR of intermediary metabolism: implications for systemic physiology. Annual Review of Physiology. 63:15 – 48.

Sonoda S, Spee C, Barron E, Ryan SJ, Kannan R, Hinton DR. (2009). A protocol for the culture and differentiation of highly polarized human retinal pigment epithelial cells. Nat Protoc. 4(5):662-73.

Steele, F.R., Chader, G.J., Johnson, L.V., and Tombran-Tink, J. (1992). Pigment epithelium-derived factor: Neurotrophic activity and identification as a member of the serine protease inhibitor gene family. Proceedings of the National Academy of Sciences of the United States of America 90: 1526-1530.

Sterling, P. and Matthews, G. (2005). Structure and function of ribbon synapses. Trends in Neurosciences. 28(1): 20 – 29.

Strauss, O. (2005). The Retinal Pigment Epithelium in Visual Function. Physiological Reviews 85:845-881.

Strumilo, E. (1995). Effect of Ca2+ on the activity of mitochondrial NADP-specific isocitrate dehydrogenase from rabbit adrenals. Acta Biochimica Polonica. 42(3): 325 – 328.

Sutherland, E.W., and Wosilait, W.D. (1955). Inactivation and activation of liver phosphorylase. Nature. 175:169 – 170.

Sutherland, E.W., and Wosilait, W.D. (1956). The relationship of epinephrine and glucagon to liver phosphorylase. I. Liver phosphorylase; preparation and properties. Journal of Biological Chemistry. 218:459 – 468.

Suzuki, A., Stern, S.A., Bozdagi, O., Huntley, G.W., et al. (2013). Astorcyte-neuron lactate transport is required for long-term memory formation. Cell. 144: 810 – 823.

Swarup, A., Samuels, I.S., Bell, B.A., Han, J.Y.S., Du, J., et al. (2018). Modulating GLUT1 expression in the retinal pigment epithelium decreases glucose levels in the retina: impact on photoreceptors and Müller glial cells. American Journal of Cell Physiology. 316: C121 – C133.

Terluk MR, Kapphahn RJ, Soukup LM, Gong H, Gallardo C, Montezuma SR, et al. (2015). Investigating mitochondria as a target for treating age-related macular degeneration. J Neurosci. 35(18):7304-11.

Thoreson, W.B., and Witkovsky, P. (1999). Glutamate Receptors and Circuits in the Vertebrate Retina. Progress in Retinal and Eye Research 18(6): 765-810.

Uhlén, M., Fagerberg, L., Hallström, B.M., Lindskog, C., Oksvold, P., Mardinoglu, A., Sivertsson, Å., Kampf, C., Sjöstedt, E., Asplund, A., et al. (2015). Proteomics. Tissue-based map of the human proteome. Science *347*, 1260419–1260419.

Venkatesh A, Ma S, Le YZ, Hall MN, Ruegg MA, Punzo C. (2015). Activated mTORC1 promotes long-term cone survival in retinitis pigmentosa mice. J Clin Invest. 125(4):1446-58.

Wang L, Tornquist P, Bill A. (1997). Glucose metabolism in pig outer retina in light and darkness. Acta Physiol Scand. 160(1):75-81.

Wang, W., Lee, S.J., Scott, P.A., Ross, J.W., Kaplan, H.J., Dean, D.C. 2016. Two-Step Reactivation of Dormant Cones in Retinitis Pigmentosa. Cell. 15: 1-14.

Warburg O, Posener, K., Negrelein, E. (1924). On the metabolism of carcinoma cells. Bioschemische Zeitschrift. 152:309-44.

Wei H, Xun Z, Granado H, Wu A, Handa JT. (2016). An easy, rapid method to isolate RPE cell protein from the mouse eye. Exp Eye Res. 145:450-5.

Whitmore SS, Wagner AH, DeLuca AP, Drack AV, Stone EM, Tucker BA, et al. (2014).Transcriptomic analysis across nasal, temporal, and macular regions of human neural retina and RPE/choroid by RNA-Seq. Exp Eye Res. 129:93-106.

Winkler BS. (1981). Glycolytic and oxidative metabolism in relation to retinal function. J Gen Physiol. 77(6):667-92.

Wohl SG, Reh TA. (2016). The microRNA expression profile of mouse Muller glia in vivo and in vitro. Sci Rep. 6:35423.

Wright, E.M. (2013). Glucose transport families SLC5 and SLC50. Molecular Aspect of Medicine. 34:183-196.

Wright, E.M., Loo, D.D.F., and Hirayama, B.A. (2011). Biology of Human Sodium Glucose Transporters. Physiol Rev. 91: 733-794.

Yoon, H., Fanelli, A., Grollman, E.F., and Philp, N.J. (1997). Identification of a Unique Moncarboxylate Transporter (MCT3) in Retinal Pigment Epithelium. Biochemical and Biophysical Research Communications 234:90-94.

Yoshioka K, Takahashi H, Homma T, Saito M, Oh KB, Nemoto Y, et al. (1996). A novel fluorescent derivative of glucose applicable to the assessment of glucose uptake activity of Escherichia coli. Biochim Biophys Acta. 1289(1):5-9.

Zhao F, and Keating A.F. (2007). Functional Properties and Genomics of Glucose Transporters. Current Genomics. 8:113-128.

Zhao C, Yasumura D, Li X, Matthes M, Lloyd M, Nielsen G, et al. (2011). mTOR-mediated dedifferentiation of the retinal pigment epithelium initiates photoreceptor degeneration in mice. J Clin Invest. 121(1):369-83.

Zhang L, Du J, Justus S, Hsu CW, Bonet-Ponce L, Wu WH, et al. (2016). Reprogramming metabolism by targeting sirtuin 6 attenuates retinal degeneration. J Clin Invest. 126(12):4659-73.

Zhu, S., Yam, M., Wang, Y., Linton, J.D., Grenell, A., Hurley, J.B., Du, J. (2018). Impact of euthanasia, dissection and postmortem delay on metabolic profile in mouse retina and RPE/choroid. Exp Eye Research. 174:113 – 120.